



This is a repository copy of *Severe zinc depletion of escherichia coli: roles for high affinity zinc binding by ZinT, zinc transport and zinc-independent proteins* .

White Rose Research Online URL for this paper:
<http://eprints.whiterose.ac.uk/9031/>

Article:

Graham, A.I., Hunt, S., Stokes, S.L. et al. (5 more authors) (2009) Severe zinc depletion of escherichia coli: roles for high affinity zinc binding by ZinT, zinc transport and zinc-independent proteins. *Journal of Biological Chemistry*, 284 (27). pp. 18377-18389. ISSN 0021-9258

<https://doi.org/10.1074/jbc.M109.001503>

Reuse

Unless indicated otherwise, fulltext items are protected by copyright with all rights reserved. The copyright exception in section 29 of the Copyright, Designs and Patents Act 1988 allows the making of a single copy solely for the purpose of non-commercial research or private study within the limits of fair dealing. The publisher or other rights-holder may allow further reproduction and re-use of this version - refer to the White Rose Research Online record for this item. Where records identify the publisher as the copyright holder, users can verify any specific terms of use on the publisher's website.

Takedown

If you consider content in White Rose Research Online to be in breach of UK law, please notify us by emailing eprints@whiterose.ac.uk including the URL of the record and the reason for the withdrawal request.



eprints@whiterose.ac.uk
<https://eprints.whiterose.ac.uk/>

promoting access to White Rose research papers



Universities of Leeds, Sheffield and York
<http://eprints.whiterose.ac.uk/>

This is an author produced version of a paper published in **Journal of Biological Chemistry**.

White Rose Research Online URL for this paper:
<http://eprints.whiterose.ac.uk/9031>

Published paper

Graham, A.I., Hunt, S., Stokes, S.L., Bramall, N., Bunch, J., Cox, A.G., McLeod, C.W., Poole, R.K. (2009) *Severe zinc depletion of escherichia coli: roles for high affinity zinc binding by ZinT, zinc transport and zinc-independent proteins*, Journal of Biological Chemistry, 284 (27), pp. 18377-18389

<http://dx.doi.org/10.1074/jbc.M109.001503>

1 **SEVERE ZINC DEPLETION OF ESCHERICHIA COLI: ROLES FOR HIGH-AFFINITY**
2 **ZINC BINDING BY ZinT, ZINC TRANSPORT AND ZINC-INDEPENDENT PROTEINS**

3 Alison I. Graham¹, Stuart Hunt¹, Sarah L. Stokes², Neil Bramall², Josephine Bunch^{2#}, Alan
4 G. Cox², Cameron W. McLeod² and Robert K. Poole^{1*}

5 ¹Department of Molecular Biology and Biotechnology and ²Centre for Analytical Sciences, The
6 University of Sheffield, Western Bank, Sheffield, S10 2TN, UK

7 Running title: Transcriptional response to zinc limitation

8 Address correspondence to: Robert Poole, Department of Molecular Biology and Biotechnology
9 The University of Sheffield, Western Bank, Sheffield, S10 2TN, UK; Telephone (0)114 222
10 4447; Fax (0)114 222 2800; E-mail r.poole@sheffield.ac.uk.

11 # Present address: School of Chemistry, University of Birmingham, Edgbaston, Birmingham,
12 B15 2TT, UK.
13
14

15 Zinc ions play indispensable roles in
16 biological chemistry. However, bacteria
17 have an impressive ability to acquire
18 Zn²⁺ from the environment, making it
19 exceptionally difficult to achieve Zn²⁺
20 deficiency and so a comprehensive
21 understanding of the importance of
22 Zn²⁺ has not been attained. Reduction of
23 the Zn²⁺ content of Escherichia coli
24 growth medium to 60 nM or less is
25 reported here for the first time, without
26 recourse to chelators of poor specificity.
27 Cells grown in Zn²⁺-deficient medium
28 had a reduced growth rate and
29 contained up to five times less cellular
30 Zn²⁺. To understand global responses to
31 Zn²⁺ deficiency, microarray analysis
32 was conducted of cells grown under
33 Zn²⁺-replete and Zn²⁺-depleted
34 conditions in chemostat cultures. Nine
35 genes were up-regulated more than two-
36 fold (P<0.05) in cells from Zn²⁺-deficient
37 chemostats, including zinT (yodA). zinT
38 is shown to be regulated by Zur (zinc
39 uptake regulator). A mutant lacking
40 zinT displayed a growth defect and a
41 three-fold lowered cellular Zn²⁺ level
42 under Zn²⁺ limitation. The purified
43 ZinT protein possessed a single, high-
44 affinity metal-binding site which can
45 accommodate Zn²⁺ or Cd²⁺. A further
46 up-regulated gene, ykgM, is believed to
47 encode a non-Zn²⁺-finger-containing
48 paralogue of the Zn²⁺-finger ribosomal
49 protein L31. The gene encoding the
50 periplasmic Zn²⁺-binding protein znuA
51 showed increased expression. During

52 both batch and chemostat growth, cells
53 “found” more Zn²⁺ than was originally
54 added to the culture, presumably due to
55 leaching from the culture vessel. Zn²⁺
56 elimination is shown to be a more
57 precise method of depleting Zn²⁺ than
58 by using the chelator N, N, N', N'-
59 tetrakis(2-

60 pyridylmethyl)ethylenediamine (TPEN).
61 Almost all biological interactions
62 depend upon contacts between precisely
63 structured protein domains and Zn²⁺ may
64 be used to facilitate correct folding and
65 stabilize the domain (1,2). Zn²⁺ also plays
66 an indispensable catalytic role in many
67 proteins (1). Although normally classed as
68 a trace element, Zn²⁺ accumulates to the
69 same levels as Ca and Fe in the
70 Escherichia coli cell (3); predicted Zn²⁺-
71 binding proteins account for 5-6% of the
72 total proteome (4).

73 However, despite its indispensable
74 role in biology, as with all metals, Zn²⁺ can
75 become toxic if accumulated to excess.
76 With no sub-cellular compartments to
77 deposit excess metal, Zn²⁺ homeostasis in
78 bacteria relies primarily on tightly
79 regulated import and export mechanisms
80 (5). The major inducible high-affinity Zn²⁺
81 uptake system is the ABC transporter,
82 ZnuABC. ZnuA is important for growth
83 (6) and Zn²⁺ uptake (7) and is thought to
84 pass Zn²⁺ to ZnuB for transport through
85 the membrane. Zn²⁺-bound Zur represses
86 transcription of znuABC, whilst addition of
87 the metal chelator N, N, N', N'-tetrakis(2-
88 pyridylmethyl)ethylenediamine (TPEN)

89 de-represses expression from a
90 promoterless lacZ gene inserted into znuA,
91 znuB and znuC (8). Zur can sense sub-
92 femtomolar concentrations of cytosolic
93 Zn^{2+} , implying that cellular Zn^{2+} starvation
94 commences at exceptionally low Zn^{2+}
95 concentrations (3). Outten and O'Halloran
96 (3) found that the minimal Zn^{2+} content
97 required for growth in *E. coli* is 2×10^5
98 atoms per cell, which corresponds to a
99 total cellular Zn^{2+} concentration of 0.2
100 mM, approximately 2000 times the Zn^{2+}
101 concentration found in the medium. A
102 similar cellular concentration of Zn^{2+} was
103 found in cells grown in Luria-Bertani
104 medium (LB).

105 Thus, *E. coli* has an impressive
106 ability to acquire and concentrate Zn^{2+} (3),
107 making the task of depleting this organism
108 of Zn^{2+} very difficult. Nevertheless, during
109 the course of this work, a paper was
110 published (9) in which the authors
111 conclude that ZinT (formerly YodA) "is
112 involved in periplasmic zinc binding and
113 either the subsequent import or shuttling
114 of zinc to periplasmic zinc-containing
115 proteins under zinc-limiting conditions".
116 Surprisingly, this conclusion was drawn
117 from experiments in which Zn^{2+} levels in
118 the medium were lowered only by
119 reducing the amount of Zn^{2+} added,
120 without metal extraction or chelation.

121 Only a few attempts have been
122 made to study the global consequences of
123 metal deficiency using "omic"
124 technologies. A study using TPEN (10)
125 found 101 genes to be differentially-
126 regulated in *E. coli*. However, the authors
127 note that TPEN has been reported to bind
128 Cd^{2+} , Co^{2+} , Ni^{2+} and Cu^{2+} more tightly
129 than it binds Zn^{2+} and, indeed, 34 of the
130 101 differentially-regulated genes are
131 transcriptionally regulated by Fur (the Fe-
132 uptake regulator) or involved in Fe or Cu
133 metabolism. Thus the transcriptome of *E.*
134 *coli* associated with Zn^{2+} deficiency alone
135 has not been elucidated. Most genome-
136 wide microarray studies of the effects of
137 metal stresses to date have been carried
138 out in batch culture, but continuous culture
139 offers major benefits for such studies. The

140 greater biological homogeneity of
141 continuous cultures and the ability to
142 control all relevant growth conditions,
143 such as pH and especially growth rate,
144 eliminate the masking effects of secondary
145 stresses and growth rate changes, allowing
146 more precise delineation of the response to
147 an individual stress (11,12). In the case of
148 transcriptomics, it has been demonstrated
149 that the reproducibility of analyses
150 between different laboratories is greater
151 when chemostat cultures are used than
152 when identical analyses are performed
153 with batch cultures (13). Some studies
154 have exploited continuous culture to
155 examine the effects of metal stresses such
156 as that of Lee et al. (14) in which *E. coli*
157 cultures grown in continuous culture at a
158 fixed specific growth rate, temperature and
159 pH were used to assay the transcriptional
160 response to Zn^{2+} excess. In the
161 present study, *E. coli* was grown in
162 continuous culture in which severe
163 depletion was achieved without recourse
164 to chelating agents in the medium by
165 thorough extraction and scrupulous
166 attention to metal contamination.
167 Microarray analysis identifies only nine
168 genes that respond significantly to Zn^{2+}
169 starvation. We demonstrate here for the
170 first time that one such gene, zinT, is up-
171 regulated in response to extreme Zn^{2+}
172 deprivation by Zur, and that ZinT has a
173 high affinity for Zn^{2+} . We also reveal
174 roles for Zn^{2+} re-distribution in surviving
175 Zn^{2+} deficiency.

176

177 **EXPERIMENTAL PROCEDURES**

178

179 Bacterial strains and growth conditions -
180 Bacterial strains used in this study are
181 listed in Table 1. Cells were grown in
182 glycerol-glycerophosphate medium
183 (GGM), slightly modified from Beard et
184 al. (15). GGM is buffered with 2-(N-
185 morpholino)ethanesulfonic acid (MES),
186 which has minimal metal-chelating
187 properties, and uses organic phosphate as
188 the phosphate source to minimise
189 formation of insoluble metal phosphates
190 (16). Final concentrations are: MES (40.0

191 mM), NH₄Cl (18.7 mM), KCl (13.4
192 mM), β-glycerophosphate (7.64 mM),
193 glycerol (5.00 mM), K₂SO₄ (4.99 mM),
194 MgCl₂ (1.00 mM), EDTA (134 μM),
195 CaCl₂·2H₂O (68.0 μM), FeCl₃·6H₂O (18.5
196 μM), ZnO (6.14 μM), H₃BO₃ (1.62 μM),
197 CuCl₂·2H₂O (587 nM), Co(NO₃)₂·6H₂O
198 (344 nM), and (NH₄)₆Mo₇O₂₄·4H₂O (80.9
199 nM) in MilliQ water (Millipore). Bulk
200 elements (MES, NH₄Cl, KCl, K₂SO₄ and
201 glycerol in MilliQ water at pH 7.4 (batch
202 growth) or 7.6 (continuous culture)) were
203 passed through a column containing
204 Chelex-100 ion exchange resin (Bio-Rad)
205 to remove contaminating cations. Trace
206 elements (with or without Zn²⁺ as
207 necessary) and a CaCl₂ solution were then
208 added to give the final concentrations
209 shown above prior to autoclaving. After
210 autoclaving, MgCl₂ and β-
211 glycerophosphate were added at the final
212 concentrations shown. All chemicals were
213 of AnalaR grade purity or higher. Chelex-
214 100 was packed into a Bio-Rad Glass
215 Econo-column (approximately 120 mm ×
216 25 mm) that had previously been soaked in
217 3.5% nitric acid for 5 d.
218 Creating Zn²⁺-deficient conditions and
219 establishing Zn²⁺-limited cultures -
220 Culture vessels and medium were depleted
221 of Zn²⁺ by extensive acid-washing of
222 glassware, the use of a chemically-defined
223 minimal growth medium, chelation of
224 contaminating cations from this medium
225 using Chelex-100, and the use of newly-
226 purchased high-purity chemicals and
227 metal-free pipette tips. Plastics that came
228 into contact with the medium (e.g. bottles,
229 tubes, tubing) were selected on the basis of
230 their composition and propensity for metal
231 leaching, and included polypropylene,
232 polyethylene, polytetrafluoroethylene
233 (PTFE) or polyvinyl chloride (PVC).
234 Dedicated weigh boats, spatulas,
235 measuring cylinders, PTFE-coated stir
236 bars and a pH electrode were used. PTFE
237 face masks, polyethylene gloves and a
238 PTFE-coated thermometer were also used.
239 Solutions were filter-sterilised using
240 polypropylene syringes with no rubber

241 seal, in conjunction with syringe filters
242 with a PTFE membrane and polypropylene
243 housing. Vent filters contained a PTFE
244 membrane in polypropylene housing. Cells
245 were grown in continuous culture in a
246 chemostat that was constructed entirely of
247 non-metal parts as detailed below.
248 Continuous culture of E. coli strain
249 MG1655 - E. coli strain MG1655 was
250 grown in custom-built chemostats made
251 entirely of non-metal parts essentially as in
252 Lee et al. (14) with some modifications.
253 Glass growth vessels and flow-back traps
254 were soaked extensively (approximately
255 two months) in 10% nitric acid before
256 rinsing thoroughly in MilliQ water. Vent
257 filters (Vent Acro 50 from VWR) were
258 connected to the vessel using PTFE
259 tubing. Metal-free pipette tips were used
260 (MAXYMum Recovery Filter Tips from
261 Axygen). Culture volume was maintained
262 at 120 ml using an overflow weir in the
263 chemostat vessel (14). The vessel was
264 inoculated using one of the side-arms.
265 Flasks were stirred on KMO 2 Basic IKA-
266 Werke stirrers at 437 rpm determined
267 using a handheld laser tachometer
268 (Compact Instruments Ltd). The use of a
269 vortex impeller suspended from above the
270 culture avoided grinding of the glass
271 vessel that would occur if a stir bar were
272 used. Samples were taken from the culture
273 vessel as in Lee et al. (14). The dilution
274 rate (and hence the specific growth rate)
275 was 0.1 h⁻¹ (which is below the maximal
276 specific growth rate μ_{max} for this strain
277 (17)). No washout was observed in long-
278 term chemostat cultures in Zn²⁺-depleted
279 medium. One chemostat was fed medium
280 that contained “adequate” Zn²⁺ (i.e. normal
281 GGM concentration), whilst the other
282 contained no added Zn²⁺ and had been
283 depleted of Zn²⁺ as above. Chemostats
284 were grown for 50 h to allow five culture
285 volumes to pass through the vessel and
286 allow an apparent (pseudo-)steady state to
287 be reached. More prolonged growth was
288 avoided to minimise the formation of
289 mutations in the rpoS gene (18). Samples
290 were taken throughout to check pH, OD₆₀₀,
291 glycerol content and for contaminants.

292 Steady state values for pH and OD₆₀₀ were
293 6.9 and 0.6, respectively. Glycerol assays
294 (19) showed cultures to be glycerol-
295 limited.

296 The “Zn²⁺-free” chemostat was
297 inoculated with cells that had been sub-
298 cultured in Zn²⁺-free medium. A 0.25 ml
299 aliquot of a saturated culture of strain
300 MG1655 grown in LB was centrifuged
301 and the pellet used to inoculate 5 ml of
302 GGM that was incubated overnight at 37
303 °C with shaking. A 2.4 ml (i.e. 2% of
304 chemostat volume) aliquot of this was then
305 used to inoculate the chemostat. The
306 “adequate Zn²⁺” chemostat was inoculated
307 with cells treated in essentially the same
308 way but grown in GGM containing
309 “adequate” Zn²⁺. The two cultures (+/-
310 Zn²⁺) used to inoculate the chemostats had
311 OD₆₀₀ readings within 2.5% of each other.
312 Aliquots from the chemostat were used to
313 harvest RNA and for metal analysis by
314 inductively coupled plasma-atomic
315 emission spectroscopy (ICP-AES, see
316 below).

317 Batch growth of E. coli strains in GGM
318 +/- Zn²⁺ - A saturated culture was grown
319 in LB (with antibiotics as appropriate). To
320 minimise carry-over of broth, cells were
321 collected from approximately 0.25 ml
322 culture by centrifugation and the pellet
323 resuspended in a 5 ml GGM starter culture
324 (with Zn²⁺ and antibiotics as appropriate)
325 for 24 h. Side-arm flasks containing 25 ml
326 GGM with Zn²⁺ were then inoculated with
327 the equivalent of 1 ml of a culture with
328 OD₆₀₀ of 0.6. For these experiments, “plus
329 Zn” cultures were grown in medium
330 containing adequate Zn²⁺ where no special
331 precautions were taken in preparing the
332 medium. “Zn-depleted” cultures were
333 grown in side-arm flasks that had been
334 soaked extensively in 10% nitric acid
335 before rinsing thoroughly in MilliQ water.
336 Growth was measured over several hours
337 using a Klett colorimeter and a red filter
338 (number 66; Manostat Corporation). The
339 colorimeter was blanked using GGM. No
340 antibiotics were present in the growth
341 medium used for batch growth curves as
342 they can act as chelators (20-23), but

343 cultures were spotted onto solid LB plates
344 with and without antibiotics at the end of
345 the growth curve to verify that antibiotic
346 resistance was retained. At the end of the
347 growth curve, aliquots of the culture were
348 combined and pelleted for ICP-AES
349 analysis (see below).

350 RNA isolation and microarray procedures
351 - These were conducted as described by
352 Lee et al. (14). RNA was quantified using
353 a BioPhotometer (Eppendorf). E. coli K-
354 12 V2 OciChip microarray slides were
355 purchased from Ocimum Biosolutions Ltd
356 (previously MWG Biotech). Biological
357 experiments (i.e. comparison of low Zn²⁺
358 versus adequate Zn²⁺ in chemostat culture)
359 were carried out three times, and a dye
360 swap performed for each experiment,
361 providing two technical repeats for each of
362 the three biological repeats. Data were
363 analysed as before (14). Spots
364 automatically flagged as bad, negative or
365 poor in the Imagen software were
366 removed before the statistical analysis was
367 carried out in GeneSight.

368 zinT gene inactivation - The zinT gene
369 was functionally inactivated by the
370 insertion of a chloramphenicol resistance
371 cassette using the method of Datsenko and
372 Wanner (24). The pACYC184
373 chloramphenicol resistance cassette was
374 amplified by PCR using primers that have
375 40 bases of identity at their 5' ends to
376 regions within the zinT gene. The forward
377 primer was 5'-
378 GCATGGTCATCACTCACACGGCAAA
379 CCCTTAACAGAGGTCAAGCCACTGG
380 AGCACCTCAA-3' and the reverse was
381 5'-

382 CAATGCCGTCCTCAATGCCAATCAT
383 CTCGATATCTGTTGCACGGGGAGAG
384 CCTGAGCAA-3' (regions homologous
385 to zinT are underlined). The linear DNA
386 was used to transform strain RKP5082 by
387 electroporation. This strain contains
388 pKD46 which over-expresses the phage λ
389 recombination enzymes when arabinose is
390 present. Bacteria were grown to an OD₆₀₀
391 of 0.6 in 500 ml LB containing ampicillin
392 (150 µg/ml final concentration) and
393 arabinose (1 mM final concentration) at 30

394 °C. Cells were then pelleted and made
395 electrocompetent by washing the pellet
396 three times in ice-cold 10% glycerol. The
397 last pellet was not resuspended but
398 vortexed into a slurry. Aliquots of cells
399 (50-100 µl) were electroporated with 1-
400 10% linear DNA (v:v) at 1800 V. Cells
401 were recovered by the addition of 1 ml of
402 LB and incubation at 37 °C for 90 min.
403 Cells were then pelleted and plated onto
404 LB containing chloramphenicol at 34
405 µg/ml (final concentration). Loss of
406 pKD46 plasmid was checked by streaking
407 transformants on LB agar plates
408 containing ampicillin (150 µg/ml final
409 concentration). Insertion of the
410 chloramphenicol cassette was checked by
411 DNA sequencing. The *zinT::cam* mutant
412 strain was named RKP5456.

413 Construction of a $\lambda\Phi(P_{zinT}\text{-lacZ})$ *zur::Spc^r*
414 strain - The *zur::Spc^r* mutation in strain
415 SIP812 (8) was moved into strain AL6,
416 which harbours the $\lambda\Phi(P_{zinT}\text{-lacZ})$ fusion
417 (25), by P1 transduction (26). The strain
418 was named RKP5475.

419 Quantitative real-time-polymerase chain
420 reaction (qRT-PCR) - This was carried out
421 on RNA samples harvested from the
422 chemostats exactly as described in Lee et
423 al. (14). The mRNA levels of *holB* were
424 unchanged as determined by array analysis
425 and were thus used as an internal control.

426 ICP-AES - Cells (from 25 ml culture
427 (batch) or approximately 85 ml
428 (chemostat)) were harvested by
429 centrifugation at 5000 × g for 5 min
430 (Sigma 4K15) in polypropylene tubes
431 from Sarstedt (catalogue numbers
432 62.547.004 (50 ml) or 62.554.001 (15
433 ml)). Culture supernatants were retained
434 for analysis. Pellets were washed three
435 times in 0.5 ml of 0.5 % HNO₃ (Aristar
436 nitric acid, 69% v/v) to remove loosely
437 bound elements. Supernatants collected
438 from the washes were also retained for
439 analysis.

440 Pellets were resuspended in 0.5 ml
441 HNO₃ (69%) before transfer to nitric acid-
442 washed test tubes (previously dried). The
443 samples were placed in an ultrasonic bath

444 for approximately 30 min to break the
445 cells. The resultant digest was then
446 quantitatively transferred to a calibrated 15
447 ml tube and made up to 5 ml with 1%
448 HNO₃. Samples were analysed using a
449 Spectrociros^{CCD} (Spectroanalytical)
450 inductively coupled plasma-atomic
451 emission spectrometer using background
452 correction. Analyte curves were created
453 for each element to be tested using multi-
454 element standard solutions containing 0.1,
455 0.2, 1, 5 and 10 mg l⁻¹. The wavelengths
456 (nm) for each element were as follows:
457 Ca, 183.801; Co, 228.616; Cu, 324.754
458 and 327.396; Fe, 259.941; Mg, 279.079;
459 Mo, 202.030; Na, 589.592; Zn, 213.856. A
460 1% nitric acid solution in MilliQ water
461 was used as a blank and to dilute cell
462 digests before ICP-AES analysis.
463 Concentrations of each element in each
464 sample (pellets, culture supernatants and
465 wash supernatants) were calculated using
466 the standard curves. Measurements
467 obtained were the mean of five replicate
468 integrations. The limit of Zn²⁺ detection
469 was 0.001 mg l⁻¹ (i.e. 1 ppb). In the
470 “simple” low-matrix solutions analysed
471 here, the wavelength used for Zn²⁺
472 detection is interference-free and specific
473 for Zn²⁺.

474 Elemental recoveries were
475 calculated from these samples. Two
476 different recovery calculations were
477 performed: 1) the percentage of an
478 element in the culture that was
479 subsequently recovered in the washed cell
480 pellet, wash supernatants and culture
481 supernatant, and 2) the percentage of an
482 element recovered in the unwashed pellet
483 and culture supernatant. The former was
484 used for batch and chemostat samples and
485 the latter for chemostat only. In some
486 samples, element concentrations were
487 below the calculated limit of detection
488 (LOD) for the method. LOD is calculated
489 from the calibration curve based on three
490 σ of a blank signal. Where the signal is at
491 or below the LOD, the instrument reports
492 a <LOD value. In these cases, the LOD is
493 used in subsequent calculations so will be
494 an over-estimation. Detection of Zn²⁺ was

495 further complicated because, in many
496 cases, Zn²⁺ concentrations were close to
497 unavoidable background levels.

498 Calculation of dry cell weight – Cellular
499 metal contents were expressed on a dry
500 cell mass basis. This was determined by
501 filtering known volumes of culture (10 ml,
502 20 ml and 30 ml) through pre-weighed
503 cellulose nitrate filters, 47 mm diameter
504 and pore size 0.2 µm (Millipore). The
505 filters had previously been dried at 105 °C
506 for 18-24 h to constant weight. The filters
507 were again dried at 105 °C until a constant
508 weight was attained, which was recorded.

509 β-galactosidase activity assay - For β-
510 galactosidase assays with strains AL6
511 (λΦ(P_{zinT}-lacZ)) and RKP5475, a saturated
512 culture was grown in LB with or without
513 spectinomycin (50 µg/ml final
514 concentration) as appropriate and cells
515 from approximately 0.25 ml culture
516 collected and resuspended in 5 ml GGM
517 with or without Zn²⁺ and spectinomycin as
518 appropriate. This was incubated overnight
519 at 37 °C with shaking. A 1 ml aliquot of
520 this was then used to inoculate several
521 cultures (15 ml) as described in the text.
522 Cultures were harvested when an OD₆₀₀ of
523 0.2-0.4 was reached. Immediately prior to
524 harvesting, 5 µl was spotted onto solid LB
525 plates with and without antibiotics to
526 check that resistance was retained.
527 Separate flasks were set up and used to
528 grow the strains under each of the
529 conditions mentioned above for ICP-AES
530 analysis.

531 β-galactosidase activity was
532 measured in CHCl₃- and SDS-
533 permeabilized cells by monitoring the
534 hydrolysis of o-nitrophenyl-β-D-
535 galactopyranoside. Cell pellets were
536 resuspended in approximately 15 ml Z
537 buffer (26). Each culture was assayed in
538 triplicate. Absorbance (A) at 420 nm, 550
539 nm and 600 nm was measured to allow β-
540 galactosidase activity (Miller units) to be
541 calculated as (26).

542 Cloning of zinT for protein purification -
543 Primers 5'-
544 CTCCTGCCTTTCATATGGGTCATCA

545 C-3' (forward) and 5'-
546 CATAGTGATGAGCTCGTCTGTAGC-
547 3' (reverse) were used to amplify the zinT
548 coding region minus the sequence that
549 encodes the 24-amino acid periplasmic
550 signalling sequence (27) from MG1655
551 genomic DNA. An NdeI site was
552 engineered into the forward primer and a
553 SacI site into the reverse primer
554 (underlined above), which, following
555 enzymic digestion, allowed the 684 bp
556 product to be ligated into pET28a
557 (Novagen). The translated protein is
558 produced with an N-terminal His-tag and
559 thrombin cleavage site. This allowed the
560 protein to be purified using TALON metal
561 affinity resin (Clontech), which uses
562 immobilised Co²⁺ ions to trap
563 polyhistidine-tags with high-affinity,
564 followed by cleavage with thrombin to
565 release the pure protein. Insertion of the
566 correct fragment was verified by digestion
567 with restriction endonucleases. pET28a
568 containing the zinT gene fragment
569 (pET28a-zinT) was used to transform E.
570 coli over-expression strain BL21(DE3)
571 pLysS and named strain RKP5466.
572 Over-expression and purification of
573 recombinant ZinT – Strain RKP5466 was
574 grown in LB containing kanamycin (50
575 µg/ml, to maintain pET28a-zinT) and
576 chloramphenicol (34 µg/ml, to maintain
577 pLysS) at 37 °C with shaking to an OD₆₀₀
578 of 0.6, at which point IPTG was added to a
579 final concentration of 1 mM. Cells were
580 harvested after a further 4 h incubation.
581 Pellets were stored at -80 °C for later use;
582 a cell pellet derived from 1 l culture was
583 re-suspended in approximately 15 ml of
584 buffer P (50 mM Tris/MOPS, 100 mM
585 KCl, pH 8) and sonicated on ice to break
586 the cells. Cell debris was pelleted by
587 centrifugation for 30 min at 12 000 × g at
588 4 °C, whereupon the supernatant was
589 removed and further centrifuged for 15
590 min at 27 000 × g. The cleared lysate was
591 then loaded into a 5 ml TALON resin
592 column, washed with 50 ml buffer P,
593 followed by 50 ml buffer P containing 20
594 mM imidazole. Thrombin (60-80 units in
595 3-4 ml buffer P) was pipetted onto the

596 column, allowed to soak into the resin and
597 incubated overnight at room temperature.
598 Ten 1-ml fractions were eluted using
599 buffer P. Recombinant ZinT was
600 determined to be >95% pure by sodium
601 dodecyl sulphate-polyacrylamide gel
602 electrophoresis (SDS-PAGE). Protein was
603 quantified using its absorbance at 280 nm
604 and the theoretical extinction coefficient of
605 $35995 \text{ M}^{-1} \text{ cm}^{-1}$ (estimated using the web-
606 based program ProtParam at ExPASy
607 (<http://ca.expasy.org/cgi-bin/protparam>),
608 which assumes that all cysteines in the
609 protein appear as half-cysteines using
610 information based on (28). The theoretical
611 extinction coefficient is based on the
612 protein sequence minus the periplasmic
613 targeting sequence.
614 N-terminal protein sequencing –
615 Following SDS-PAGE, purified YodA
616 was blotted onto a polyvinylidene fluoride
617 (PVDF) membrane. The fragment of
618 interest was excised from the membrane
619 and the sequence determined using an
620 Applied Biosystems Procise 392 protein
621 sequencer.
622 Assays of metal binding to purified ZinT -
623 Purified recombinant ZinT was exchanged
624 into buffer D (20 mM MOPS pH 7) using
625 a PD-10 desalting column (GE
626 Healthcare). ZinT (1 ml) was incubated
627 with various concentrations of
628 $\text{ZnSO}_4 \cdot 7\text{H}_2\text{O}$ (ACS grade reagent) and/or
629 $\text{CdCl}_2 \cdot 2\frac{1}{2}\text{H}_2\text{O}$ (AnalaR grade) for 1 h at
630 room temperature. The protein/metal
631 mixture was then loaded onto a PD-10
632 column and eluted in 7×0.5 ml fractions
633 using buffer D. Fractions were assayed for
634 A_{280} and for metal content using ICP-AES.
635 Quantification of some elements was
636 below the LOD in a limited number of
637 samples that do not affect the overall
638 interpretation of the experiment. In these
639 cases the value for the LOD was used for
640 subsequent calculations and thus will be
641 an over-estimation.
642 Mag-fura-2 binding experiments - Purified
643 recombinant ZinT was exchanged into
644 buffer M (140 mM NaCl, 20 mM Hepes,
645 pH 7.4) using a PD-10 desalting column.
646 Absorption spectra were collected using a

647 Varian Cary 50 Bio UV-visible
648 spectrophotometer at 37°C . Buffer
649 composition and experimental conditions
650 were taken from Simons (1993). ZinT
651 (500 μl ; approximately 15 μM) was placed
652 in a quartz cuvette and a spectrum taken
653 from which the concentration of ZinT was
654 determined. Difference spectra were
655 recorded in which the reference sample
656 was buffer M. Equimolar mag-fura-2 (MF;
657 Molecular Probes, catalogue number M-
658 1290) was then added. Aliquots of
659 $\text{ZnSO}_4 \cdot 7\text{H}_2\text{O}$ (ACS grade reagent) and/or
660 $\text{CdCl}_2 \cdot 2\frac{1}{2}\text{H}_2\text{O}$ (AnalaR grade) in buffer M
661 were added, mixed and incubated for 1
662 min before collecting spectra. Equilibrium
663 was established within 1 min of Zn^{2+} being
664 added.

665 RESULTS

666
667
668 Creating Zn^{2+} -deficient conditions -
669 Several precautions, based on normal
670 analytical practice, and the findings of Kay
671 (29) regarding Zn^{2+} contamination, were
672 taken to ensure that culture vessels and
673 medium were depleted of Zn^{2+} where
674 necessary. Table 2 shows typical values
675 for the amounts of various metals in GGM
676 as analysed by ICP-AES. Both Zn^{2+} -
677 depleted and -replete media show good
678 correlation with the expected values. In
679 various batches of medium analysed, Zn^{2+}
680 concentrations in Zn^{2+} -depleted medium
681 ranged from <0.001 to 0.004 mg l^{-1} (<15
682 to 60 nM Zn^{2+}). The variation in Zn^{2+} -
683 depletion achieved is a result of the
684 difficulty in excluding Zn^{2+} from all
685 sources that come into contact with the
686 medium and culture. Sodium was used as
687 the exchanging ion on Chelex-100, but
688 excess sodium was not detected in the
689 medium following chelation (data not
690 shown).
691 Growth in Zn^{2+} -depleted batch cultures -
692 E. coli strain MG1655 was grown in GGM
693 with or without Zn^{2+} (Fig. 1A). The Zn^{2+} -
694 limited culture showed a lag in entering
695 exponential phase and a semi-logarithmic
696 analysis of growth (not shown) revealed
697 that the Zn^{2+} -limited culture had an

698 increased doubling time (159.0 min)
699 compared to the Zn²⁺-replete culture
700 (125.4 min) and reached a lower final OD.
701 Since OD measurements may reflect cell
702 size changes (30), samples were taken at
703 the end of growth for electron microscopy
704 but no discernible size difference was seen
705 between E. coli cells grown with or
706 without Zn²⁺ in GGM (not shown). Cells
707 grown in GGM (+/- Zn²⁺) were, however,
708 smaller (length, width and volume) than
709 cells grown in rich medium (LB),
710 presumably due to a slower growth rate
711 (31).

712 GGM contains EDTA, which
713 prevents precipitation of the trace elements
714 present. This is well-established and
715 common practice (17). However, to
716 investigate whether this EDTA was itself
717 creating Zn²⁺ depletion, we cultured
718 MG1655 in GGM with and without EDTA
719 (Supp. Fig. 1). When grown in GGM
720 without EDTA, MG1655 displayed a
721 longer lag phase and reduced growth yield.
722 The growth rate was also affected; the
723 doubling time during exponential growth
724 increased from 125.5 min (with EDTA) to
725 131.5 min (without EDTA). Thus, EDTA
726 is not creating a state of “Zn²⁺-depletion”
727 but rather is a beneficial component of the
728 medium.

729 As well as growing at a reduced
730 rate, cells grown in Zn²⁺-depleted medium
731 had approximately 1.8- to 5.0-fold less
732 cellular Zn²⁺ than those grown in Zn²⁺
733 replete medium (based on three separate
734 experiments). For example, at the end of
735 the growth curve shown in Fig. 1A, the
736 cells cultured in Zn²⁺-replete medium
737 contained 1.12×10^{-5} mg Zn²⁺/mg dry
738 weight cells and the cells grown in Zn²⁺-
739 depleted medium contained 3.40×10^{-6} mg
740 Zn²⁺/mg dry weight cells (a 3.3-fold
741 difference). Here, “cellular Zn” is defined
742 as that which cannot be removed by three
743 successive washes with 0.5% nitric acid.
744 To verify the reliability of the metal
745 analyses, elemental recoveries were
746 calculated from these samples. Fig. 2
747 shows that, for cells grown in Zn²⁺-replete
748 medium, Zn²⁺ recovery was between 90

749 and 110%, and, for cells grown in Zn²⁺-
750 replete and Zn²⁺-deplete medium, the
751 recovery of Fe, Cu, Co and Mg was also
752 between 90 and 110%. For these elements,
753 therefore, the metal content in the washed
754 pellet and the culture supernatant and the
755 wash supernatants fully accounts for the
756 metal initially added to the culture in the
757 medium. However, this was not true for
758 Zn²⁺ recovery in cells grown in Zn²⁺-
759 deficient medium. Zn²⁺ in these cells,
760 together with that in the culture
761 supernatant and wash supernatants, was 5-
762 fold higher than the amount originally
763 added to the culture in the medium. This
764 suggests an avid Zn²⁺-sequestering ability
765 of cells cultured under limiting Zn²⁺
766 conditions. Details of the analyses of
767 individual pellets, wash solutions,
768 supernatants and media for Zn²⁺ are found
769 in Supp. Table 1. We conclude that Zn²⁺
770 limitation can be achieved in batch culture
771 without resorting to chelators despite
772 effective bacterial Zn²⁺ scavenging
773 mechanisms.

774 *Cells grown in continuous culture “find”*
775 *extra Zn²⁺ -* To explore Zn²⁺ acquisition
776 and localization at constant growth rates
777 and defined conditions for a detailed
778 transcriptomic study, E. coli strain
779 MG1655 was grown in parallel glycerol-
780 limited chemostats, one fed with medium
781 that contained “adequate” Zn²⁺ and one
782 that had been rigorously depleted of Zn²⁺.
783 For the majority of elements assayed (Fe,
784 Cu, Co, Mg, Mo, K, Mg, Na, P, S), the
785 percentage recoveries were 90-110%
786 (data not shown). However, more Zn²⁺ was
787 recovered from the cells grown in the
788 Zn²⁺-deficient chemostat than was
789 originally added to the culture (Table 3),
790 as in batch culture (Fig. 2). This is
791 presumed to be due to active leaching
792 from glassware or carry-over from the
793 inoculum. Interestingly, this percentage
794 markedly decreased with successive
795 experiments in the same chemostat
796 apparatus, suggesting that there is less
797 Zn²⁺ able to be leached after repeated runs
798 of culture in the same chemostat vessel
799 (Table 3). Details of the analyses of

800 individual pellets, wash solutions,
801 supernatants and media are found in Supp.
802 Table 2.

803 Cells grown in the Zn^{2+} -deficient
804 chemostat consistently contained less
805 cellular Zn^{2+} than those grown in Zn^{2+} -
806 replete medium (e.g. 2.94×10^{-5} mg
807 Zn^{2+} /mg cells for cells grown in adequate
808 Zn^{2+} and 0.536×10^{-5} mg Zn^{2+} /mg cells for
809 cells harvested from run 5 of the Zn^{2+} -
810 limited chemostat (a 5.5-fold decrease)).

811 Transcriptome changes induced by Zn^{2+}
812 deficiency - The genome-wide mRNA
813 changes of strain MG1655 grown in
814 continuous culture with adequate or
815 limiting Zn^{2+} were probed using
816 microarray technology. Commonly
817 applied criteria to determine significance
818 in transcriptomic studies are a fold-change
819 of more than two and a P value of less
820 than 0.05. Using these criteria, of the
821 4288 genes arrayed, only nine showed
822 significant changes (an increase in all
823 cases) in mRNA levels and are listed in
824 Table 4. Genes not meeting these criteria
825 may be biologically significant but are not
826 studied further here. It should be noted
827 that microarrays measure relative
828 abundance of mRNA but cannot inform as
829 to whether changes occur because of
830 changes in the rate of transcription or
831 because of changes in the stability of the
832 transcript. Zn^{2+} has been reported to affect
833 the stability of the mRNA of a human Zn^{2+}
834 transporter (32). The full dataset has been
835 deposited in GEO (accession number
836 GSE11894) (33). Three genes were chosen
837 for further study based on known links to
838 Zn^{2+} homeostasis. The remaining six genes
839 were not studied further. In total, 21 genes
840 displayed a greater than two-fold increase
841 in mRNA levels, 13 displayed a decrease
842 and the mRNA changes from 140 genes
843 had a P value of <0.05 . No genes
844 exhibited a two-fold or greater decrease in
845 mRNA levels with a P value of less than
846 0.05.

847 The gene exhibiting the greatest
848 change in transcription (and lowest P
849 value) was *zinT* (up-regulated 8.07-fold),
850 previously known as *yodA*. *ZinT* was

851 initially identified in a global study of *E.*
852 *coli* defective in the histone-like nucleoid-
853 structuring protein H-NS (34). Levels of
854 *ZinT* increase when cells are grown in the
855 presence of Cd^{2+} (27), and at pH 5.8 (35).
856 More recently, it has been suggested that
857 the abundance of *yodA* mRNA changes in
858 response to cytoplasmic pH stress (36).
859 Transcription of *zinT* is increased by the
860 addition of Cd^{2+} , but not Zn^{2+} , Cu^{2+} , Co^{2+}
861 and Ni^{2+} , to growing cells (25), even
862 though Cd^{2+} , Zn^{2+} and Ni^{2+} were found in
863 crystals of *ZinT* (37,38) (see discussion).
864 Further evidence for the binding of Cd^{2+} to
865 *ZinT* was presented by Stojnev et al. (39),
866 who found that γ -labelled $^{109}Cd^{2+}$ -bound
867 proteins could be detected in wild-type *E.*
868 *coli* but not a mutant lacking *zinT* (39),
869 suggesting a specific role for *ZinT* in Cd^{2+}
870 accumulation. *ZinT* is found primarily in
871 the cytoplasm in unstressed cells but is
872 exported to the periplasm upon Cd^{2+} stress
873 (25). The mature, periplasmic form of
874 *ZinT* is thought to form a disulfide bond,
875 as it is a substrate of *DsbA* (40). A recent
876 paper (9) suggests a role for *ZinT* in
877 periplasmic zinc binding under zinc-
878 limiting conditions but no direct evidence
879 for *zinT* up-regulation in response to
880 rigorous exclusion of zinc has been
881 previously reported.

882 The *znuA* gene was also up-
883 regulated in response to Zn^{2+} depletion
884 (Table 4). *ZnuA* is the soluble periplasmic
885 metallochaperone component of the
886 *ZnuABC* Zn^{2+} importer and was up-
887 regulated 2.88-fold. In this complex, *ZnuB*
888 is the integral membrane protein and *ZnuC*
889 is the ATPase component. The *znuB* and
890 *znuC* genes were up-regulated by 1.34-
891 and 1.36-fold respectively (with P values
892 of >0.05 and thus are not shown in Table
893 4). No other genes that encode proteins
894 involved in Zn^{2+} transport (specifically
895 *zupT*, *zur*, *zitB*, *zntA*, *zntR*, *zraS*, *zraR*,
896 *zraP*) were more than 1.4-fold up-
897 regulated or 1.2-fold down-regulated and
898 all had P values of >0.05 . The changes in
899 the mRNA levels of a number of genes
900 involved in Zn^{2+} metabolism are shown in
901 Table 5.

902 The *ykgM* gene was up-regulated
903 2.64-fold in this study (Table 4) and has
904 been identified previously by
905 bioinformatics as the non-Zn²⁺-ribbon-
906 containing paralogue of the ribosomal
907 protein L31 that normally contains a Zn²⁺-
908 ribbon motif and is thus predicted to bind
909 Zn²⁺ (41). Panina et al. (41) predicted (but
910 did not show) that *ykgM* would be up-
911 regulated upon Zn²⁺ starvation and then
912 displace the Zn²⁺-containing version of
913 L31 in the ribosome, thus liberating Zn²⁺
914 for use by Zn²⁺-containing enzymes.
915 However, no previous study has attained
916 the degree of Zn²⁺ limitation reported here
917 and the role of *ykgM* has not been further
918 explored.

919 To verify the results obtained by
920 microarray experiments, several genes that
921 were induced by Zn²⁺ depletion were
922 examined by qRT-PCR to determine
923 independently relative mRNA levels. The
924 levels of up-regulation determined by
925 qRT-PCR (mean ± normalised standard
926 deviation) were as follows: *yodA*, 7.77 ±
927 0.63; *ykgM*, 2.83 ± 0.61; and *znuA*, 2.34 ±
928 0.58. These values correspond closely to
929 increases in the microarray analysis of
930 8.07-, 2.64-, 2.88-fold respectively.
931 Similar qRT-PCR values were obtained on
932 one (*ykgM* and *znuA*) or two (*yodA*) other
933 occasions. The mRNA levels of *holB*
934 (internal control) were unchanged as
935 determined by qRT-PCR and array
936 analysis.

937 Hypersensitivity of selected strains to Zn²⁺
938 deficiency - To assess the importance of
939 the *ykgM*, *zinT* and *znuA* genes in
940 surviving Zn²⁺ deficiency, mutants were
941 used in which each gene are inactivated by
942 insertion of an antibiotic resistance
943 cassette; the growth of these isogenic
944 strains was compared in Zn²⁺-depleted and
945 Zn²⁺ replete liquid cultures (Fig. 1). Each
946 strain (wild-type and mutants) grew more
947 poorly in the absence of Zn²⁺ than in its
948 presence. Also, in Zn²⁺-depleted medium,
949 the *ykgM::kan*, *zinT::cam* and *znuA::kan*
950 mutants consistently grew more poorly
951 than MG1655 in the same medium. We
952 were unable to culture the *znuA::kan*

953 mutant to >5 Klett units in the severely
954 Zn²⁺-depleted conditions achieved here
955 (Fig. 1D). All experiments were carried
956 out in triplicate and similar results were
957 seen on at least two separate occasions.
958 We confirmed by qRT-PCR that the genes
959 downstream of *ykgM*, *zinT* and *znuA* (i.e.
960 *ykgO*, *yodB* and *yebA*, respectively) were
961 in all cases transcribed in the mutant
962 strains.

963 We measured cellular Zn²⁺ levels
964 in bacteria grown in conditions of severe
965 Zn²⁺ limitation in batch culture. The levels
966 of Zn²⁺ detected in cell digests on analysis
967 by ICP-AES were exceedingly low.
968 Nevertheless, the *zinT::cam* strain
969 contained approximately 9-fold less
970 cellular Zn²⁺ when cultured under Zn²⁺
971 limitation (1.28 × 10⁻⁶ mg Zn²⁺/mg cells)
972 than when grown in Zn²⁺-replete (1.16 ×
973 10⁻⁵ mg Zn²⁺/mg cells) conditions. Also,
974 under Zn²⁺-deficient conditions, the
975 *zinT::cam* strain contained nearly 3-fold
976 less cellular Zn²⁺ than MG1655 wild-type
977 cells grown under similar conditions (1.28
978 × 10⁻⁶ mg Zn²⁺/mg cells and 3.40 × 10⁻⁶
979 mg Zn²⁺/mg cells, respectively). These
980 data are the first to demonstrate a role for
981 *ZinT* in Zn²⁺ acquisition under strictly
982 Zn²⁺-limited conditions. When the
983 *znuA::kan* mutant was assayed after
984 growth in Zn²⁺ depleted conditions, the
985 measurement of cellular Zn²⁺ was below
986 the LOD. Similar results were seen on at
987 least one other occasion.

988 Transcriptional regulation of *zinT* under
989 various Zn²⁺ concentrations - Having
990 established that *zinT* transcription was
991 elevated on Zn²⁺ depletion, a P_{*zinT*}-*lacZ*
992 transcriptional fusion (25), in which *lacZ*
993 is transcribed from the *zinT* promoter, was
994 used to investigate an alternative Zn²⁺
995 removal method and the effects of added
996 Cd²⁺ and Zn²⁺. Fig. 3A shows that
997 λΦ(P_{*zinT*}-*lacZ*) activity was highly up-
998 regulated under the Zn²⁺-deficient
999 conditions created here (in which Zn²⁺ is
1000 excluded from the medium). These data
1001 were compared with cultures treated with
1002 TPEN (Fig. 3B), which is widely used as a
1003 Zn²⁺ chelator (e.g. (3,7,42-45)). Fig. 3B

1004 shows that expression from $\lambda\Phi$ (P_{zinT} -lacZ)
1005 increases with increasing TPEN
1006 concentrations in the growth medium.
1007 Although expression from $\lambda\Phi$ (P_{zinT} -lacZ)
1008 was higher in cells grown in medium
1009 containing TPEN than in cells grown in
1010 adequate Zn^{2+} , it was lower than that of
1011 cells grown in medium from which Zn^{2+}
1012 has been rigorously eliminated (Fig. 3A).
1013 In LB medium, the P_{zinT} -lacZ fusion strain
1014 has previously been shown to respond to
1015 elevated levels of Cd^{2+} but not of Zn^{2+}
1016 (25). In GGM, the construct was again
1017 unresponsive to elevated Zn^{2+} but no
1018 response was seen to elevated Cd^{2+} (Fig.
1019 3A), although this may be due to
1020 difficulties in growing cells at high levels
1021 of Cd^{2+} , which were near its maximum
1022 permissive concentration.

1023 A Zur-binding site has been
1024 reported in the *zinT* promoter (41), and
1025 Zn^{2+} -bound Zur represses the transcription
1026 of *znuABC* (8). Therefore, to test the
1027 hypothesis that Zur also negatively-
1028 regulates *zinT*, $\lambda\Phi$ (P_{zinT} -lacZ) activity was
1029 monitored in a strain lacking *zur*. Fig. 3C-
1030 D shows that, in a *zur* mutant, $\lambda\Phi$ (P_{zinT} -
1031 lacZ) activity was not dependent on the
1032 extracellular Zn^{2+} concentration under any
1033 condition tested. Thus, Zur is a negative
1034 regulator of *zinT* transcription.

1035 Stoichiometric binding of Zn^{2+} and Cd^{2+} by
1036 ZinT - To investigate the possible role of
1037 ZinT in metal binding as suggested by the
1038 transcription and growth studies reported
1039 here, the *zinT* gene was cloned into
1040 pET28a such that the translated protein
1041 lacked the periplasmic signal sequence but
1042 was fused to a polyhistidine tag and
1043 thrombin cleavage site to aid purification.
1044 The polyhistidine tag was removed by
1045 cleavage with thrombin to minimise the
1046 danger of the protein adopting aberrant
1047 conformations. The sequence of the
1048 resultant protein, which was used to
1049 calculate the extinction coefficient, mimics
1050 the form of the protein found in the
1051 periplasm. Residual imidazole in the final
1052 ZinT preparation was avoided by using
1053 only a single wash step containing

1054 imidazole (20 mM) during purification,
1055 and exchange into a buffer lacking
1056 imidazole before final use. Effective
1057 removal of the polyhistidine tag was
1058 confirmed by N-terminal sequencing. The
1059 pure recombinant protein (Fig. 4A) was
1060 incubated with different molar ratios of
1061 Zn^{2+} , and then subjected to size exclusion
1062 chromatography to assess co-elution of
1063 Zn^{2+} with ZinT. Fig. 4 shows the elution
1064 profiles of ZinT and Zn^{2+} following
1065 incubation of ZinT with 0, 0.25, 0.5, 1 and
1066 2 molar equivalents of Zn^{2+} . Fig. 4B (and
1067 Fig. 5A-D) shows that, even when no Zn^{2+}
1068 is added, ZinT co-eluted from the size
1069 exclusion column with Zn^{2+} . The
1070 occupancy of Zn^{2+} observed under these
1071 conditions (0.6 mol Zn^{2+} /mol ZinT) was
1072 approximately half that observed at super-
1073 stoichiometric Zn^{2+} /ZinT ratios (Fig. 4F)
1074 and so we conclude that the Zn^{2+} content
1075 shown in Fig. 4B represents approximately
1076 0.5 Zn^{2+} per ZinT. This suggests a high
1077 affinity of ZinT for Zn^{2+} and is reminiscent
1078 of the crystallisation of ZinT (38): crystals
1079 formed in the absence of added metals
1080 contained Zn^{2+} or Ni^{2+} , indicative of high
1081 metal affinity (see Discussion). When
1082 ZinT was incubated with 0.25 or 0.5 molar
1083 equivalents of Zn^{2+} (Fig. 4C-D) more Zn^{2+}
1084 co-eluted with ZinT than was originally
1085 added. However, when 1 (Fig. 4E), 2 (Fig.
1086 4F) or 3 (data not shown) molar
1087 equivalents Zn^{2+} were incubated with
1088 ZinT, approximately one equivalent eluted
1089 from the column with the protein. These
1090 data provide evidence that ZinT binds 1
1091 Zn^{2+} ion with high affinity.

1092 Previous work (38) has suggested
1093 that ZinT is able to bind Cd^{2+} and so the
1094 experiment was also carried out using
1095 Cd^{2+} . ZinT co-elutes from a size exclusion
1096 column with up to 1 molar equivalent of
1097 Cd^{2+} , even when initially incubated with
1098 more (Fig. 5A-D). When 13.3 nmol ZinT
1099 was incubated without Cd^{2+} prior to size
1100 exclusion chromatography, the eluate
1101 contained less than 18 pmol Cd^{2+} per
1102 fraction (not shown). It should be noted
1103 that, in the case of Cd^{2+} , the Cd^{2+} /ZinT
1104 ratio was approximately 0.9 but never

1105 exceeded 1 (Fig. 5D) unlike the case with
1106 Zn^{2+} (Fig. 4F). This is attributable to the
1107 inevitable contamination of reagents and
1108 materials with Zn^{2+} but not Cd^{2+} .

1109 To investigate competition of Zn^{2+}
1110 and Cd^{2+} for site(s) in ZinT, the protein
1111 was incubated with both metals and co-
1112 elution of metals and protein assayed.
1113 ZinT co-eluted with almost 1 molar
1114 equivalent of Zn^{2+} and approximately 0.5
1115 molar equivalents of Cd^{2+} (Fig. 5E). These
1116 ratios were similar when the $Cd^{2+}:Zn^{2+}$
1117 ratio was increased to 2:1 (Fig. 5F),
1118 indicating that ZinT preferentially binds
1119 Zn^{2+} over Cd^{2+} . Multi-element analysis of
1120 the eluate also revealed approximately 0.5
1121 molar equivalents of Co^{2+} with ZinT. This
1122 was seen in all experiments and the
1123 reasons for this are discussed below. Two
1124 metal ions per ZinT protein would match
1125 previous structural data (38).

1126 Mag-fura-2 (MF) and ZinT competitive
1127 metal binding - To estimate the affinity of
1128 ZinT for Zn^{2+} , Mag-fura-2, a chromophore
1129 that binds Zn^{2+} in a 1:1 ratio (46) and with
1130 a K_d of 20 nM (47), was used. Its
1131 absorption maximum shifts from 366 nm
1132 to 325 nm on Zn^{2+} binding, which is
1133 accompanied by a decrease in its
1134 extinction coefficient from 29900 $M^{-1} cm^{-1}$
1135 (MF) to 1880 $M^{-1} cm^{-1}$ (Zn^{2+} -MF) (46).
1136 Therefore Zn^{2+} binding to MF can be
1137 tracked by examining the absorbance at
1138 366 nm (Fig. 6A). Fig. 6B shows a
1139 titration of a 1:1 ZinT:MF mixture (filled
1140 circles) and MF alone (open circles) with
1141 Zn^{2+} . When ZinT was not present, the
1142 ΔA_{366} decreased to zero when 1 molar
1143 equivalent of Zn^{2+} had been added. When
1144 ZinT was present, however, incremental
1145 additions of Zn^{2+} gave smaller decreases in
1146 MF absorbance reaching a plateau at 2
1147 molar equivalents of Zn^{2+} . This provides
1148 good evidence that, although the affinity
1149 of ZinT for Zn^{2+} is not high enough to
1150 completely outstrip MF of Zn^{2+} , ZinT
1151 competes with MF for binding of Zn^{2+} .
1152 The K_d for Zn^{2+} binding by ZinT is
1153 therefore not less than 20 nM, but of an
1154 order that is able to compete with MF for
1155 Zn^{2+} .

1156 MF also binds Cd^{2+} in a 1:1 ratio
1157 and has a K_d for Cd^{2+} of 126 nM (48).
1158 Addition of Cd^{2+} to MF and ZinT (Fig.
1159 6C-D) elicited a smaller decrease in
1160 absorbance than with MF alone, again
1161 indicating the ability of ZinT to compete
1162 with MF for Cd^{2+} . Without protein, the
1163 decrease in absorbance at 366 nm
1164 plateaued at 1 molar equivalent of metal
1165 added whereas, when ZinT was present,
1166 this shifted to 2. These data together
1167 suggest that ZinT has one binding site for
1168 metal that can be occupied by Cd^{2+} or Zn^{2+}
1169 and that the site has a sufficiently low K_d
1170 to be able to compete with MF for these
1171 metals.

1172

1173

DISCUSSION

1174

1175 The manipulation of metal ion
1176 concentrations in biological systems, so
1177 that the consequences of metal excess and
1178 limitation may be studied, is a major
1179 challenge. Global responses to elevated
1180 levels of Ag^{2+} , Cd^{2+} , Cu^{2+} , Ni^{2+} , Zn^{2+} and
1181 As (14,49-54) have been reported.
1182 However, constituents of complex growth
1183 medium can bind to metal ions and result
1184 in the metal ion concentration available to
1185 the cells being orders of magnitude lower
1186 than that added (16). For the first time, we
1187 have grown Zn^{2+} -depleted E. coli in batch
1188 and chemostat culture in defined medium,
1189 without recourse to chelating agents, and
1190 defined the transcriptome associated with
1191 severe Zn^{2+} limitation. In batch culture,
1192 wild-type E. coli MG1655 cells grown in
1193 Zn^{2+} -depleted cultures showed an
1194 increased doubling time (Fig. 1A) and a
1195 reduction in Zn^{2+} content compared to
1196 Zn^{2+} -replete cultures. Thus, in the face of
1197 extreme Zn^{2+} depletion in the extracellular
1198 medium, homeostatic mechanisms ensure
1199 adequate cellular Zn contents.

1200 Zn^{2+} -depleted medium was
1201 successfully prepared by eliminating Zn^{2+}
1202 during medium preparation and culture. In
1203 contrast, chelators can be unspecific, strip
1204 metals from exposed sites and increase the
1205 availability of certain metals (16). The
1206 major disadvantage of using chelators is

1207 that the metal is still present in the
1208 medium to be picked up by proteins with a
1209 higher affinity for the metal than that
1210 exhibited by the chelator. For example,
1211 ZnuA is able to compete with EDTA for
1212 Zn²⁺ (6). Fig. 3A highlights the
1213 disadvantage of using chelators to study
1214 Zn²⁺ deficiency; the widely-used chelator
1215 TPEN was less effective than Zn²⁺
1216 elimination, as judged by $\lambda\Phi(P_{zinT}\text{-lacZ})$
1217 activity. Although neither are specific to
1218 Zn²⁺, both TPEN and EDTA have been
1219 used in studies focussing on Zn²⁺-
1220 depletion (see earlier references and (55)).

1221 Fig. 2 and Table 3 show that cells
1222 grown in Zn²⁺-depleted medium
1223 accumulate Zn²⁺ that cannot be accounted
1224 for by the medium constituents. Table 3
1225 shows that the extent of leaching
1226 decreased with successive experiments in
1227 the same chemostat apparatus. The most
1228 likely explanation is that metal is actively
1229 leached from the glassware (flasks or
1230 chemostat vessel). Kay (29) notes that acid
1231 washing removes only surface Zn²⁺, which
1232 can be replaced from deeper within the
1233 glass. Previous studies have shown that
1234 growing cells in medium deficient in one
1235 nutrient can lead to cells evolving
1236 mechanisms to increase uptake of that
1237 nutrient (56).

1238 In contrast to (10), this study
1239 found only nine genes to be differentially
1240 regulated in response to Zn²⁺ starvation
1241 after careful metal avoidance and
1242 extraction. The small number of
1243 differentially-regulated genes suggests
1244 that, due to the ubiquity of Zn²⁺ in the
1245 environment, cells have not evolved
1246 elaborate mechanisms to cope with
1247 extreme Zn²⁺ deficiency. Interestingly,
1248 computational analysis found only three
1249 candidate Zur sites in the E. coli genome
1250 and these were immediately upstream of
1251 three genes identified here – zinT, ykgM
1252 and znuA (41).

1253 There is a precedent in Bacillus
1254 for re-distribution of Zn²⁺ under conditions
1255 of Zn²⁺ starvation, involving the synthesis
1256 of non-Zn²⁺-finger homologues of Zn²⁺-
1257 binding ribosomal proteins. Makarova et

1258 al. (57) searched sequenced genomes and
1259 found that genes encoding some ribosomal
1260 proteins were present as two copies: one,
1261 designated C⁺, contains a Zn²⁺-binding
1262 motif and, a second, designated C⁻, in
1263 which this motif is missing. In the case of
1264 the E. coli ribosomal protein L31, the C⁺
1265 form is encoded by rpmE and the C⁻ form
1266 by ykgM (41) identified in the present
1267 study. Based on the present results, we
1268 hypothesise that non-Zn²⁺-containing L31
1269 proteins displace the Zn²⁺-containing form
1270 in ribosomes and subsequent degradation
1271 of the latter form would release Zn²⁺ for
1272 use by other proteins. The number of
1273 ribosomes in the cell would make this a
1274 significant Zn²⁺ reserve. Such a model has
1275 been experimentally proven for L31
1276 proteins in Bacillus subtilis (58,59) and
1277 Streptomyces coelicolor (60,61).

1278 The present study shows that zinT
1279 expression is increased most dramatically,
1280 not by Cd²⁺ addition as reported
1281 previously (27), but by Zn²⁺ removal.
1282 However, the present and past findings are
1283 reconciled by the fact that Cd²⁺ may
1284 displace other metals from enzymes, such
1285 as Zn²⁺ from alkaline phosphatase in E.
1286 coli (2,25), so that Cd²⁺ exposure mimics
1287 Zn²⁺ depletion. Panina et al. (41) reported
1288 a Zur-binding site in the zinT promoter.
1289 Monitoring expression from $\lambda\Phi(P_{zinT}\text{-}$
1290 lacZ) in a strain lacking zur showed
1291 constitutive de-repression, regardless of
1292 extracellular Zn²⁺ concentration,
1293 confirming that Zur is involved in the
1294 regulation of zinT (Fig. 3). This was also
1295 reported in an unpublished thesis cited in a
1296 review (62).

1297 Based on the established link
1298 between ZinT and Cd²⁺, David et al. (38)
1299 included the metal (20 mM) in
1300 crystallisation trials and obtained a crystal
1301 form distinct from that obtained under
1302 crystallisation conditions that included 200
1303 mM Zn²⁺ or no added metal. The crystal
1304 structure reveals a principal metal-binding
1305 site (common to all crystallised forms) that
1306 binds one Cd²⁺ or two Zn²⁺ ions. Further
1307 metal ions are found at the protein surface
1308 at intermolecular, negatively-charged sites

1309 formed by residues from neighbouring
1310 ZinT molecules. The crystal form prepared
1311 in the absence of exogenous metal also
1312 revealed one metal ion bound in the
1313 central, common, metal-binding site; this
1314 metal was positioned similarly to Cd^{2+} and
1315 coordinated by the three same His
1316 residues. The buried metal-binding site
1317 must be of high-affinity, since no divalent
1318 cations were included in crystallisation of
1319 the native form. The binding geometry
1320 suggests that the metal in the native form
1321 is Zn^{2+} , although contamination by Ni^{2+}
1322 from the affinity chromatography or other
1323 metal ions could not be excluded, and X-
1324 ray fluorescence suggested the presence of
1325 Ni^{2+} , albeit in an unusual distorted
1326 tetrahedral geometry. Fig. 5E-F show that,
1327 in our hands, approximately 0.5 molar
1328 equivalents Co^{2+} co-elute with the ZinT
1329 protein. It is likely that this Co^{2+} has been
1330 picked up from the TALON column used
1331 during purification, again providing
1332 evidence for a high affinity metal-binding
1333 site within ZinT. No Ni^{2+} was found in
1334 eluting samples (data not shown).

1335 On the basis of the
1336 crystallography, David et al. (38) could
1337 not conclude which metal would bind to
1338 ZinT under physiological conditions. The
1339 present study shows clearly that ZinT
1340 binds both Zn^{2+} and Cd^{2+} with high
1341 affinity. The direct binding experiments
1342 (Fig. 5E-F) show that more Zn^{2+} remains
1343 bound to ZinT after size-exclusion
1344 chromatography than Cd^{2+} , providing
1345 evidence that Zn^{2+} binds to ZinT more
1346 tightly than Cd^{2+} . Also, the K_d of MF for
1347 Cd^{2+} is greater than for Zn^{2+} , so somewhat
1348 weaker binding by Cd^{2+} would not be
1349 detected in the Mag-Fura-2 competition
1350 experiments. Fig. 5E-F shows that more
1351 than 1 molar equivalent of metal can bind
1352 to the protein. This is consistent with the
1353 crystal structure proposed by David et al.
1354 (38) which suggests that at least two Zn^{2+}
1355 ions can bind in the vicinity of the high-
1356 affinity site, and that there is additional
1357 capacity for further Zn^{2+} , up to 4, although
1358 this may be due to intermolecular contacts
1359 formed during crystallization. The finding

1360 that one Zn^{2+} ion is needed to saturate the
1361 protein, as assessed by competition with
1362 Mag-Fura-2, is entirely consistent with the
1363 crystallographic data as this experiment
1364 can only report on metal binding to ZinT
1365 that is tighter than 20 nM. Although this
1366 site in ZinT accommodates different metal
1367 ions, the marked accumulation of zinT
1368 mRNA by extreme Zn^{2+} limitation strongly
1369 suggests that the physiological role of
1370 ZinT is ferrying Zn^{2+} ions in the
1371 periplasm. Indeed, David et al. (38)
1372 suggested that the binding of a second
1373 metal, possibly at a lower affinity site,
1374 could trigger a conformational change that
1375 promotes transport across the membrane
1376 or interaction with an unidentified ABC-
1377 type transporter. In support of this is the
1378 fact that ZinT shows sequence similarity
1379 to a number of periplasmic metal-binding
1380 receptors of ABC metal-transport systems
1381 that have been shown to bind Zn^{2+} .

1382 In a recent paper (9), growth in
1383 media with various Zn^{2+} supplements, or
1384 none, was purported to show “dependence
1385 of the ΔzinT mutant strain on zinc for
1386 growth”. Zn^{2+} -limited conditions were
1387 those in which reduced growth yields
1388 (OD_{595}) were observed relative to growth
1389 at 0.6-1 mM added Zn^{2+} . In defined
1390 medium containing less than 0.4 mM Zn^{2+} ,
1391 the mutant grew to lower ODs after 10 h
1392 than the wild-type but, at high Zn^{2+} (0.6-1
1393 mM), the zinT mutant grew to higher OD
1394 values than the wild-type strain. This is in
1395 conflict with the present work (Fig. 1A,
1396 C), which shows that the zinT mutant and
1397 wild-type strains grew similarly, even at
1398 only 60 nM Zn^{2+} . Surprisingly, Kershaw et
1399 al. (9) also found that even growth of the
1400 wild-type strain was impaired at low Zn^{2+}
1401 concentrations (0.4, 0.05 mM added Zn^{2+});
1402 with no added Zn^{2+} , growth was barely
1403 detectable. The claim that *E. coli* shows a
1404 strict dependence on added Zn^{2+} is, to our
1405 knowledge, unprecedented in the
1406 literature. Considerations of biomass
1407 composition suggest that the Zn^{2+}
1408 concentration in the medium used by
1409 Kershaw et al. (9) (0.5 mg l^{-1}) should
1410 support growth to a yield of 2.5 g dry

1411 weight l⁻¹ (17), well in excess of the OD₅₉₅
1412 of approximately 0.5 or lower reported (9).
1413 Furthermore, inspection of the responses
1414 of both wild-type and zinT mutant strains
1415 to metals reveals that the experiments (9)
1416 to define the Zn²⁺ response were conducted
1417 at limiting Cu concentrations: the basic
1418 defined medium contained 0.62 μM Cu
1419 (0.1 mg CuSO₄ l⁻¹), approximately 1000-
1420 fold lower than the required Cu
1421 concentration for optimal growth of both
1422 strains. Similarly, experiments to define
1423 the Cu response were conducted at
1424 limiting Zn²⁺ concentrations: the basic
1425 defined medium contained 3.1 μM Zn²⁺
1426 (0.5 mg ZnSO₄ l⁻¹), i.e. much lower than
1427 the concentration at which both strains
1428 showed reduced cell yield. These
1429 calculations may explain why the cell
1430 yields at saturating Cu concentrations
1431 (0.6–1.0 mM) were significantly lower
1432 than those at saturating Zn²⁺
1433 concentrations (0.6–1.0 mM). Thus, the
1434 data of Kershaw et al. (9) do not provide
1435 robust evidence that the zinT mutant
1436 shows a growth disadvantage at low Zn²⁺
1437 ion concentrations and conflict with
1438 previous work demonstrating the
1439 exceedingly low Cu concentrations
1440 required for Cu-limited growth (3,63).
1441 Kershaw et al. (9) reported that
1442 ZinT binds metal ions. Cd²⁺ binding was
1443 observed when Cd²⁺ was incubated with
1444 the protein in a 1:1 ratio (0.1 mM ZinT:0.1
1445 mM Cd²⁺), although the resolution of a
1446 peak corresponding to mass 22,450 (ZinT
1447 plus 1 Cd²⁺) is poor. The mass of the
1448 ZinT-Cd peak varied by 2 Da (as did the
1449 mass of apo-ZinT). The authors were only
1450 able to detect binding of Zn²⁺ to ZinT
1451 when 5 or more molar equivalents were

1452 added, although their other experiments
1453 detected binding when ZinT was incubated
1454 with less than 0.1 molar equivalents of
1455 Zn²⁺. In Fig. 4 and 5 of the present study,
1456 we show binding of Zn²⁺ to ZinT when no
1457 metal is added due to the high affinity of
1458 ZinT for contaminating Zn²⁺ in the buffers.

1459 Beside the need to sense Zn²⁺
1460 levels to maintain homeostasis for all
1461 cellular systems, lack of Zn²⁺ may be
1462 sensed by pathogens as indicative of entry
1463 into the host and, thus, trigger expression
1464 of virulence factors. Indeed, several
1465 studies in different bacteria have
1466 established that ZnuA or ZnuABC (or
1467 homologues) are required for bacterial
1468 replication in the infected host (see (55,64)
1469 amongst others).

1470 In conclusion, we propose that,
1471 when cells are severely starved of Zn²⁺,
1472 the response is to increase Zn²⁺ uptake into
1473 the cell and re-distribute non-essential
1474 Zn²⁺. The rpmE gene expresses the Zn²⁺-
1475 finger L31 protein that is incorporated into
1476 the ribosome. Upon Zn²⁺-depletion, the
1477 ykgM-encoded L31 protein is expressed
1478 (probably de-repressed by Zur) and
1479 becomes preferentially bound to the
1480 ribosome (the exact mechanism is
1481 unclear), allowing Zn²⁺ within the rpmE-
1482 encoded L31 to be recycled. The
1483 physiological role of ZinT remains to be
1484 fully established, but it may function as a
1485 Zn²⁺ chaperone to the membrane-bound
1486 Zn²⁺ importer ZnuBC (or a different
1487 importer), or mediate direct transport from
1488 the periplasm to the cytoplasm. Zn²⁺ is the
1489 metal that binds most tightly. This study
1490 provides a new appreciation of the
1491 regulation of zinT and the role of ZinT in
1492 protecting cells from Zn²⁺ depletion.

1493

1494

1495

REFERENCES

- 1496 1. Berg, J. M., and Shi, Y. (1996) *Science* **271**, 1081-1085
- 1497 2. Fraústo da Silva, J. J. R., and Williams, R. J. P. (2001) *The biological chemistry of the*
1498 *elements: the inorganic chemistry of life*, Oxford University Press, Oxford
- 1499 3. Outten, C. E., and O'Halloran, T. V. (2001) *Science* **292**, 2488-2492
- 1500 4. Andreini, C., Banci, L., Bertini, I., and Rosato, A. (2006) *J Proteome Res* **5**, 3173-3178
- 1501 5. Blencowe, D. K., and Morby, A. P. (2003) *FEMS Microbiol Rev* **27**, 291-311

- 1502 6. Berducci, G., Mazzetti, A. P., Rotilio, G., and Battistoni, A. (2004) *FEBS Lett* **569**, 289-
1503 292
- 1504 7. Patzer, S. I., and Hantke, K. (1998) *Mol Microbiol* **28**, 1199-1210
- 1505 8. Patzer, S. I., and Hantke, K. (2000) *J Biol Chem* **275**, 24321-24332
- 1506 9. Kershaw, C. J., Brown, N. L., and Hobman, J. L. (2007) *Biochem Biophys Res Commun*
1507 **364**, 66-71
- 1508 10. Sigdel, T. K., Easton, J. A., and Crowder, M. W. (2006) *J Bacteriol* **188**, 6709-6713
- 1509 11. Hayes, A., Zhang, N., Wu, J., Butler, P. R., Hauser, N. C., Hoheisel, J. D., Lim, F. L.,
1510 Sharrocks, A. D., and Oliver, S. G. (2002) *Methods* **26**, 281-290
- 1511 12. Hoskisson, P. A., and Hobbs, G. (2005) *Microbiology* **151**, 3153-3159
- 1512 13. Piper, M. D., Daran-Lapujade, P., Bro, C., Regenberg, B., Knudsen, S., Nielsen, J., and
1513 Pronk, J. T. (2002) *J Biol Chem* **277**, 37001-37008
- 1514 14. Lee, L. J., Barrett, J. A., and Poole, R. K. (2005) *J Bacteriol* **187**, 1124-1134
- 1515 15. Beard, S. J., Hashim, R., Membrillo-Hernandez, J., Hughes, M. N., and Poole, R. K.
1516 (1997) *Mol Microbiol* **25**, 883-891
- 1517 16. Hughes, M. N., and Poole, R. K. (1991) *J GenMicrobiol* **137**, 725-734
- 1518 17. Pirt, S. J. (1975) *Principles of Microbe and Cell Cultivation*, Blackwell Scientific
1519 Publications, Oxford
- 1520 18. Ferenci, T. (2007) *Adv Microb Physiol* **53**, 169-315
- 1521 19. Garland, P. B., and Randle, P. J. (1962) *Nature* **196**, 987-988
- 1522 20. Cherny, R. A., Atwood, C. S., Xilinas, M. E., Gray, D. N., Jones, W. D., McLean, C. A.,
1523 Barnham, K. J., Volitakis, I., Fraser, F. W., Kim, Y., Huang, X., Goldstein, L. E., Moir,
1524 R. D., Lim, J. T., Beyreuther, K., Zheng, H., Tanzi, R. E., Masters, C. L., and Bush, A. I.
1525 (2001) *Neuron* **30**, 665-676
- 1526 21. Lin, P. S., Kwock, L., Hefter, K., and Misslbeck, G. (1983) *Cancer Res* **43**, 1049-1053
- 1527 22. Mukherjee, G., and Ghosh, T. (1995) *J Inorg Biochem* **59**, 827-833
- 1528 23. Sebat, J. L., Paszczyński, A. J., Cortese, M. S., and Crawford, R. L. (2001) *Appl Environ*
1529 *Microbiol* **67**, 3934-3942
- 1530 24. Datsenko, K. A., and Wanner, B. L. (2000) *Proc Natl Acad Sci U S A* **97**, 6640-6645
- 1531 25. Puškárová, A., Ferianc, P., Kormanec, J., Homerova, D., Farewell, A., and Nystrom, T.
1532 (2002) *Microbiology* **148**, 3801-3811
- 1533 26. Miller, J. H. (1972) *Experiments in Molecular Genetics*, Cold Spring Harbor Laboratory
1534 Press
- 1535 27. Ferianc, P., Farewell, A., and Nystrom, T. (1998) *Microbiology* **144**, 1045-1050
- 1536 28. Gill, S. C., and von Hippel, P. H. (1989) *Anal Biochem* **182**, 319-326
- 1537 29. Kay, A. R. (2004) *BMC Physiol* **4**, 4
- 1538 30. Koch, A. L. (1961) *Biochim Biophys Acta* **51**, 429-441
- 1539 31. Neidhardt, F. C., Ingraham, J. L., and Schaechter, M. (1990) *Physiology of the Bacterial*
1540 *Cell: a Molecular Approach*, Sinauer Associates, Inc, Sunderland, Massachusetts
- 1541 32. Jackson, K. A., Helston, R. M., McKay, J. A., O'Neill, E. D., Mathers, J. C., and Ford, D.
1542 (2007) *J Biol Chem* **282**, 10423-10431
- 1543 33. Barrett, T., Troup, D. B., Wilhite, S. E., Ledoux, P., Rudnev, D., Evangelista, C., Kim, I.
1544 F., Soboleva, A., Tomashevsky, M., and Edgar, R. (2007) *Nucleic Acids Res* **35**, D760-
1545 765
- 1546 34. Laurent-Winter, C., Ngo, S., Danchin, A., and Bertin, P. (1997) *Eur J Biochem* **244**, 767-
1547 773
- 1548 35. Birch, R. M., O'Byrne, C., Booth, I. R., and Cash, P. (2003) *Proteomics* **3**, 764-776
- 1549 36. Kannan, G., Wilks, J. C., Fitzgerald, D. M., Jones, B. D., Bondurant, S. S., and
1550 Slonczewski, J. L. (2008) *BMC Microbiol* **8**, 37
- 1551 37. David, G., Blondeau, K., Renouard, M., and Lewit-Bentley, A. (2002) *Acta Crystallogr*
1552 *D Biol Crystallogr* **58**, 1243-1245

- 1553 38. David, G., Blondeau, K., Schiltz, M., Penel, S., and Lewit-Bentley, A. (2003) *J Biol*
1554 *Chem* **278**, 43728-43735
- 1555 39. Stojnev, T., Harichova, J., Ferienc, P., and Nystrom, T. (2007) *Curr Microbiol* **55**, 99-
1556 104
- 1557 40. Kadokura, H., Tian, H., Zander, T., Bardwell, J. C., and Beckwith, J. (2004) *Science* **303**,
1558 534-537
- 1559 41. Panina, E. M., Mironov, A. A., and Gelfand, M. S. (2003) *Proc Natl Acad Sci U S A* **100**,
1560 9912-9917
- 1561 42. Cai, F., Adrion, C. B., and Keller, J. E. (2006) *Infect Immun* **74**, 5617-5624
- 1562 43. Fekkes, P., de Wit, J. G., Boorsma, A., Friesen, R. H., and Driessen, A. J. (1999)
1563 *Biochemistry* **38**, 5111-5116
- 1564 44. Jackson, K. A., Helston, R. M., McKay, J. A., O'Neill E, D., Mathers, J. C., and Ford, D.
1565 (2007) *J Biol Chem* **282**, 10423-10431
- 1566 45. Scott, C., Rawsthorne, H., Upadhyay, M., Shearman, C. A., Gasson, M. J., Guest, J. R.,
1567 and Green, J. (2000) *FEMS Microbiol Lett* **192**, 85-89
- 1568 46. Yatsunyk, L. A., Easton, J. A., Kim, L. R., Sugarbaker, S. A., Bennett, B., Breece, R. M.,
1569 Vorontsov, II, Tierney, D. L., Crowder, M. W., and Rosenzweig, A. C. (2008) *J Biol*
1570 *Inorg Chem* **13**, 271-288
- 1571 47. Simons, T. J. (1993) *J Biochem Biophys Methods* **27**, 25-37
- 1572 48. de Seny, D., Heinz, U., Wommer, S., Kiefer, M., Meyer-Klaucke, W., Galleni, M., Frere,
1573 J. M., Bauer, R., and Adolph, H. W. (2001) *J Biol Chem* **276**, 45065-45078
- 1574 49. Brocklehurst, K. R., and Morby, A. P. (2000) *Microbiology* **146 (Pt 9)**, 2277-2282
- 1575 50. Kershaw, C. J., Brown, N. L., Constantinidou, C., Patel, M. D., and Hobman, J. L.
1576 (2005) *Microbiology* **151**, 1187-1198
- 1577 51. Moore, C. M., Gaballa, A., Hui, M., Ye, R. W., and Helmann, J. D. (2005) *Mol*
1578 *Microbiol* **57**, 27-40
- 1579 52. Wang, A., and Crowley, D. E. (2005) *J Bacteriol* **187**, 3259-3266
- 1580 53. Yamamoto, K., and Ishihama, A. (2005) *Mol Microbiol* **56**, 215-227
- 1581 54. Yamamoto, K., and Ishihama, A. (2005) *J Bacteriol* **187**, 6333-6340
- 1582 55. Davis, L. M., Kakuda, T., and DiRita, V. J. (2009) *J Bacteriol* **191**, 1631-1640
- 1583 56. Notley-McRobb, L., and Ferenci, T. (1999) *Environ Microbiol* **1**, 45-52
- 1584 57. Makarova, K. S., Ponomarev, V. A., and Koonin, E. V. (2001) *Genome Biol* **2**,
1585 RESEARCH 0033
- 1586 58. Akanuma, G., Nanamiya, H., Natori, Y., Nomura, N., and Kawamura, F. (2006) *J*
1587 *Bacteriol* **188**, 2715-2720
- 1588 59. Nanamiya, H., Akanuma, G., Natori, Y., Murayama, R., Kosono, S., Kudo, T.,
1589 Kobayashi, K., Ogasawara, N., Park, S. M., Ochi, K., and Kawamura, F. (2004) *Mol*
1590 *Microbiol* **52**, 273-283
- 1591 60. Owen, G. A., Pascoe, B., Kallifidas, D., and Paget, M. S. (2007) *J Bacteriol* **189**, 4078-
1592 4086
- 1593 61. Shin, J. H., Oh, S. Y., Kim, S. J., and Roe, J. H. (2007) *J Bacteriol* **189**, 4070-4077
- 1594 62. Hantke, K. (2005) *Curr Opin Microbiol* **8**, 196-202
- 1595 63. Ciccognani, D. T., Hughes, M. N., and Poole, R. K. (1992) *FEMS Microbiol Lett* **73**, 1-6
- 1596 64. Ammendola, S., Pasquali, P., Pistoia, C., Petrucci, P., Petrarca, P., Rotilio, G., and
1597 Battistoni, A. (2007) *Infect Immun* **75**, 5867-5876

FOOTNOTES

1598
1599
1600
1601 This work was supported by the Biotechnology and Biological Sciences Research Council
1602 BBSRC, UK. We thank Dr. A. J. G. Moir (Krebs Sequencing and Synthesis Facility, University
1603 of Sheffield, UK) for carrying out the N-terminal protein sequencing.

1604

1605 The abbreviations used are: Amp^r, ampicillin resistant; cam, chloramphenicol-resistance cassette;
1606 ICP-AES, inductively coupled plasma-atomic emission spectroscopy; kan, kanamycin-resistance
1607 cassette; LB, Luria-Bertani medium; LOD, limit of detection; MES, 2-(N-
1608 morpholino)ethanesulfonic acid; MF, mag-fura-2; PAGE, polyacrylamide gel electrophoresis;
1609 PTFE, polytetrafluoroethylene (Teflon[®]); PVC, polyvinyl chloride; PVDF, polyvinylidene
1610 fluoride; qRT-PCR, quantitative real-time-polymerase chain reaction; SDS, sodium dodecyl
1611 sulphate; Spc^r spectinomycin-resistance cassette; TPEN, N, N, N', N'-tetrakis(2-
1612 pyridylmethyl)ethylenediamine.

1613

1614

1615

1616

FIGURE LEGENDS

1617 **Fig. 1.** Growth of wild-type and isogenic mutant *E. coli* strains in Zn²⁺-depleted (filled circles,
1618 solid line) and Zn²⁺ replete (open circles, dashed line) GGM in batch culture. In each case, means
1619 and standard deviations of three flasks are plotted. The doubling times (min) of the strains during
1620 exponential growth, calculated from semi-logarithmic plots, were as follows: MG1655 replete,
1621 125; MG1655 deplete, 159; ykgM::kan replete, 211; ykgM::kan deplete, 885; zinT::cam replete,
1622 124; zinT::cam deplete, 193; znuA::kan replete 134; znuA::kan deplete, 492. A) MG1655 wild-
1623 type; B) ykgM::kan (FB20133); C) zinT::cam (RKP5456); D) znuA::kan (FB23354).

1624

1625

1626 **Fig. 2.** Recovery of elements following growth of strain MG1655 in batch culture. The means
1627 and standard deviations of three flasks are plotted. Black and grey bars represent the percentage
1628 of added elements recovered from cells grown in Zn²⁺-replete and -deplete conditions,
1629 respectively. See text for details of calculation.

1630

1631

1632 **Fig. 3.** β-galactosidase activity of λΦ(P_{zinT}-lacZ) under various conditions. A) and B) β-
1633 galactosidase activity of λΦ(P_{zinT}-lacZ) (strain AL6) grown in GGM containing the
1634 concentrations of Zn²⁺, Cd²⁺ and TPEN shown. The Zn²⁺ concentrations can be interpreted as
1635 follows: 6.14 μM is GGM in which the bulk elements were Chelex-100-treated and then trace
1636 elements containing Zn²⁺ were added back; <0.06 μM is GGM in which extreme precautions
1637 were taken to exclude Zn²⁺ (see text). Cultures were harvested when the OD₆₀₀ reached 0.2 - 0.4.
1638 The mean +/- standard deviation for three technical replicates is shown. The same results were
1639 seen on at least one other occasion. C) and D) β-galactosidase activity of λΦ(P_{zinT}-lacZ) in a
1640 zur::Spc^r background (strain RKP5475) grown in GGM containing the Zn²⁺ and TPEN
1641 concentrations shown. Cultures were harvested with the OD₆₀₀ reached 0.2 - 0.4. The means and
1642 standard deviations of three technical replicates are shown. The same results were seen on at
1643 least one other occasion.

1644

1645 **Fig. 4.** Metal binding to purified ZinT. A) Purified recombinant ZinT (right lane) on an SDS-
1646 PAGE gel. Size markers (left lane) are shown in kDa. Elution profiles of ZinT and Zn²⁺ from a
1647 PD-10 column following incubation of protein and metal ions. B) Elution following incubation
1648 of 13.3 nmol ZinT with no added metal. C) – F) Elution following incubation of 28.6 nmol ZinT
1649 with 0.25, 0.5, 1 or 2 molar equivalents of Zn²⁺. Filled circles with solid line, ZinT; open circles
1650 with dashed line, Zn²⁺.

1651

1652 **Fig. 5.** Elution profiles of ZinT, Zn²⁺ and Cd²⁺ from a PD-10 column following incubation of
1653 protein and metal ions. A) – D) Elution following incubation of 17.8 nmol ZinT with 0.5, 1, 2 or

1654 3 molar equivalents of Cd^{2+} . Filled circles with solid line, ZinT; open circles with dashed line,
1655 Zn^{2+} ; open triangles with dotted line, Cd^{2+} . E) – F) Elution following incubation of 13.3 nmol
1656 ZinT with 1 molar equivalent of Zn^{2+} and 1 molar equivalent of Cd^{2+} or with 1 molar equivalent
1657 of Zn^{2+} and two molar equivalents of Cd^{2+} . Filled circles with solid line, ZinT; open circles with
1658 dashed line, Zn^{2+} ; open diamonds with dotted and dashed line, Co^{2+} ; open triangles with dotted
1659 line, Cd^{2+} .

1660

1661 **Fig. 6.** Titration of ZinT and/or MF with Zn^{2+} and/or Cd^{2+} . A) Representative difference spectra
1662 (i.e. minus the protein-only spectrum) of a titration of 14.5 μM ZinT and 14.5 μM MF with Zn^{2+}
1663 (0.25 to 3.5 molar equivalents Zn^{2+} in 0.25 steps, then 4 to 6 molar equivalents in 0.5 steps).
1664 Arrows indicate the direction of absorbance changes as Zn^{2+} is added. B) Titration of 14.5 μM
1665 ZinT and 14.5 μM MF with Zn^{2+} . C) Titration of 14.3 μM ZinT and 14.3 μM MF with 1 molar
1666 equivalent of Cd^{2+} , then Zn^{2+} in 0.5 molar equivalent steps to 4 molar equivalents, then Zn^{2+} in
1667 0.5 molar equivalent steps to 6 molar equivalents. D) Titration of 14.1 μM ZinT and 14.1 μM
1668 MF with 2 molar equivalents of Cd^{2+} , then Zn^{2+} in 0.5 molar equivalent steps. In B) – D),
1669 absorbance change at 366 nm is plotted against molar equivalents of metal added. Filled circles
1670 are in the presence of ZinT; open circles are in the absence of ZinT (MF and buffer only). Lines
1671 indicate whether the added metal was Zn^{2+} or Cd^{2+} .

1672

1673

1674 **Table 1.** List of strains used.
 1675

Strain	Genotype	Source
AL6	MC4100 $\lambda\Phi(P_{zinT}\text{-lacZ})$	(25)
FB20133	MG1655 ykgM::kan	UW Genome Project
FB23354	MG1655 znuA::kan	UW Genome Project
MC4100	F ⁻ araD139 $\Delta(\text{argF-lac})$ U169 rpsL150 relA1 flbB5301 deoC1 ptsF25 rbsR	(25)
MG1655	F ⁻ λ ilvG rfb-50 rph-1	Laboratory stock
SIP812	MC4100 zur::Spc ^r	(8)
RKP5082	MG1655/pKD46 (Amp ^r)	This work
RKP5456	MG1655 zinT::cam	This work
RKP5466	BL21(DE3) pLysS pET28a-zinT	This work
RKP5475	AL6 with zur::Spc ^r	This work

1676
 1677
 1678
 1679
 1680
 1681
 1682
 1683
 1684
 1685

1686 **Table 2.** Expected and representative measured amounts of elements in Zn²⁺-sufficient and -
 1687 depleted GGM.
 1688

Element	predicted from medium composition (mg l ⁻¹)	measured by ICP-AES (mg l ⁻¹)	
		Zn ²⁺ -sufficient	Zn ²⁺ -depleted
Zn	0.401/0 (+Zn/-Zn)	0.340	0.004
Fe	1.045	0.886	0.878
Cu	0.037	0.033	0.034
Co	0.0257	0.018	0.019
Mo	0.054	0.068	0.059
Ca	2.24	2.83	2.85
Mg	24	24.2	25.0

1689
 1690
 1691
 1692
 1693
 1694
 1695
 1696
 1697
 1698
 1699

1700 **Table 3.** Recovery of Zn²⁺ from E. coli strain MG1655 growing in a Zn²⁺-limited chemostat (run
 1701 1) followed by successive cultures in the same chemostat under the same conditions (runs 2-5). A
 1702 “run” is an experiment conducted after terminating a chemostat experiment and re-establishing a
 1703 new culture in the same apparatus. ND, not determined. See text for details of calculation.
 1704

1705
 1706

Run	Recovery (%) of Zn ²⁺ in medium			
	Washed cell pellet + wash solutions + supernatant		Unwashed cell pellet + supernatant	
	+Zn	-Zn	+Zn	-Zn
1	104	1858	ND	ND
2	110	1676	ND	ND
3	105	559	ND	ND
4	104	493	102	454
5	103	248	103	254

1707
 1708
 1709
 1710
 1711
 1712
 1713
 1714
 1715
 1716

1717 **Table 4.** Genes with a significant change in mRNA level in response to Zn²⁺-deficiency. Only
 1718 genes with a fold increase of more than 2 and a P value of less than 0.05 are included. Gene
 1719 names are the primary names on Ecogene (www.ecogene.org). Gene descriptions are from
 1720 Ecogene.
 1721

Gene	b number	Gene product	Fold increase	P value (<0.05)
zinT	b1973	Periplasmic cadmium binding protein; induced by cadmium and peroxide; binds zinc, nickel, cadmium; SoxS and Fur regulated	8.07	0.0001
znuA	b1857	High-affinity ABC transport system for zinc, periplasmic	2.88	0.00117
fdnG	b1474	Formate dehydrogenase-N, selenopeptide, anaerobic; periplasmic	2.86	0.00386
emtA	b1193	Membrane-bound transglycosylase E, lipoprotein; involved in limited murein hydrolysis	2.86	0.00998
ykgM	b0296	RpmE paralog, function unknown	2.64	0.03647
mdtD	b2077	Putative transporter, function unknown; no MDR phenotype when mutated or cloned; fourth gene in mdtABCDBaeRS operon	2.46	0.01614
ribA	b1277	GTP cyclohydrolase II, riboflavin biosynthesis	2.36	0.02506
ydfE	b1577	Pseudogene, N-terminal fragment, Qin prophage	2.17	0.00452
aslA	b3801	Suppresses gpp mutants; putative arylsulfatase	2.15	0.02660

1722
 1723
 1724
 1725
 1726
 1727
 1728

1729 **Table 5.** Changes in the mRNA levels from a number of genes in response to Zn²⁺-deficiency.
 1730 Gene names are the primary names on Ecogene (www.ecogene.org). Gene descriptions are from
 1731 Ecogene.
 1732
 1733

Gene	b number	Gene product	Fold change	P value
yodB	b1974	Function unknown	2.38	0.0725
zur	b4046	Repressor for znuABC, the zinc high-affinity transport genes; dimer; binds two Zn(II) ions per monomer	1.37	0.9578
znuC	b1858	High-affinity ABC transport system for zinc	1.36	0.2294
znuB	b1859	High-affinity ABC transport system for zinc	1.34	*
zntR	b3292	Zn-responsive activator of zntA transcription	1.34	0.4857
zraS	b4003	Two component sensor kinase for ZraP; responsive to Zn ²⁺ and Pb ²⁺ ; autoregulated; regulation of Hyd-3 activity is probably due to crosstalk of overexpressed protein	1.32	0.1109
zraP	b4002	Zn-binding periplasmic protein; responsive to Zn ²⁺ and Pb ²⁺ ; regulated by zraSR two-component system; rpoN-dependent	1.25	0.9322
yiiP	b3915	Iron and zinc efflux membrane transporter; cation diffusion facilitator family; dimeric	1.17	0.2742
zitB	b0752	Zn(II) efflux transporter; zinc-inducible	1.09	0.9571
zntA	b3469	Zn(II), Cd(II), and Pb(II) translocating P-type ATPase; mutant is hypersensitive to Zn ²⁺ and Cd ²⁺ salts	1.07	0.9285
spy	b1743	Periplasmic protein induced by zinc and envelope stress, part of cpxR and baeSR regulons	1.03	0.8314
zraR	b4004	Two component response regulator for zraP; responsive to Zn ²⁺ and Pb ²⁺ ; autoregulated; regulation of Hyd-3 activity is probably due to crosstalk of overexpressed protein	0.95	0.9315
zupT	b3040	Zinc and other divalent cation uptake transporter	0.88	0.3258

1734
 1735 * Insufficient data available to obtain a P value.

Figure 1

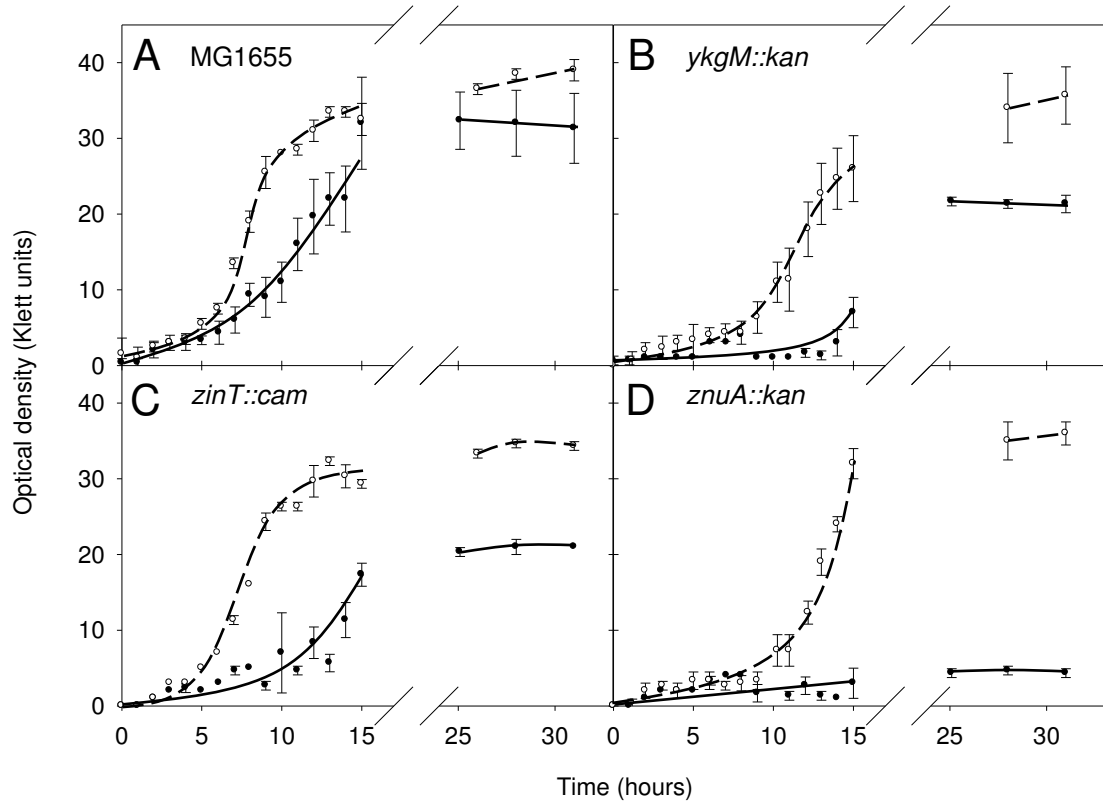


Figure 2

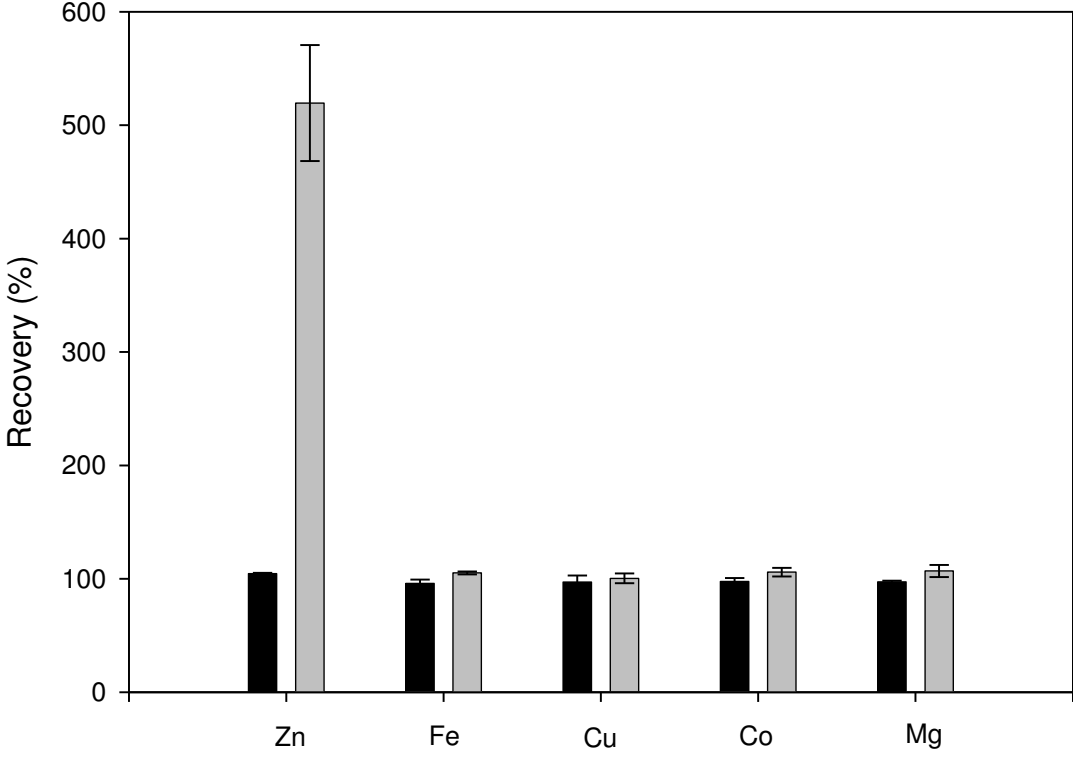


Figure 3

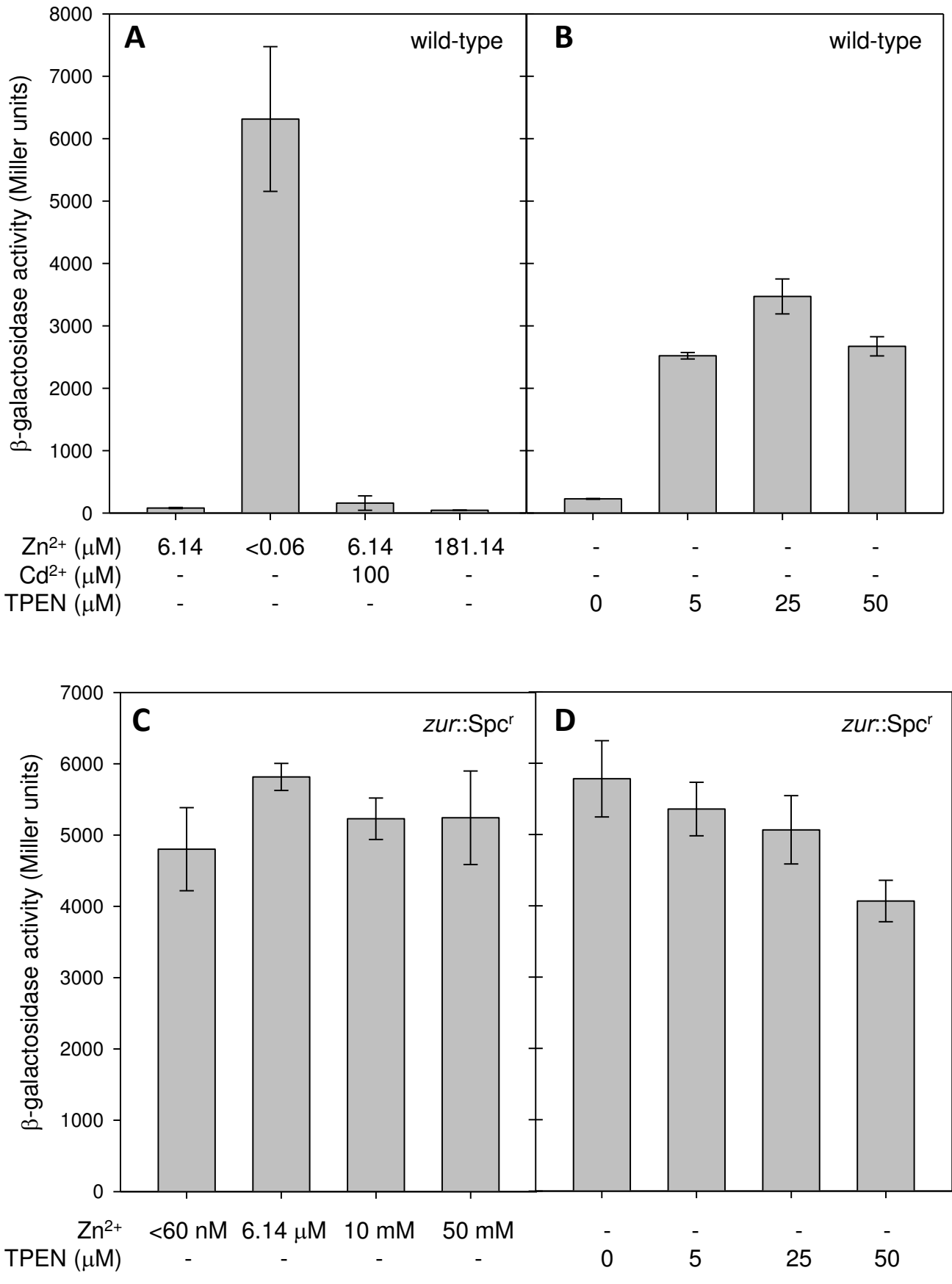


Figure 4

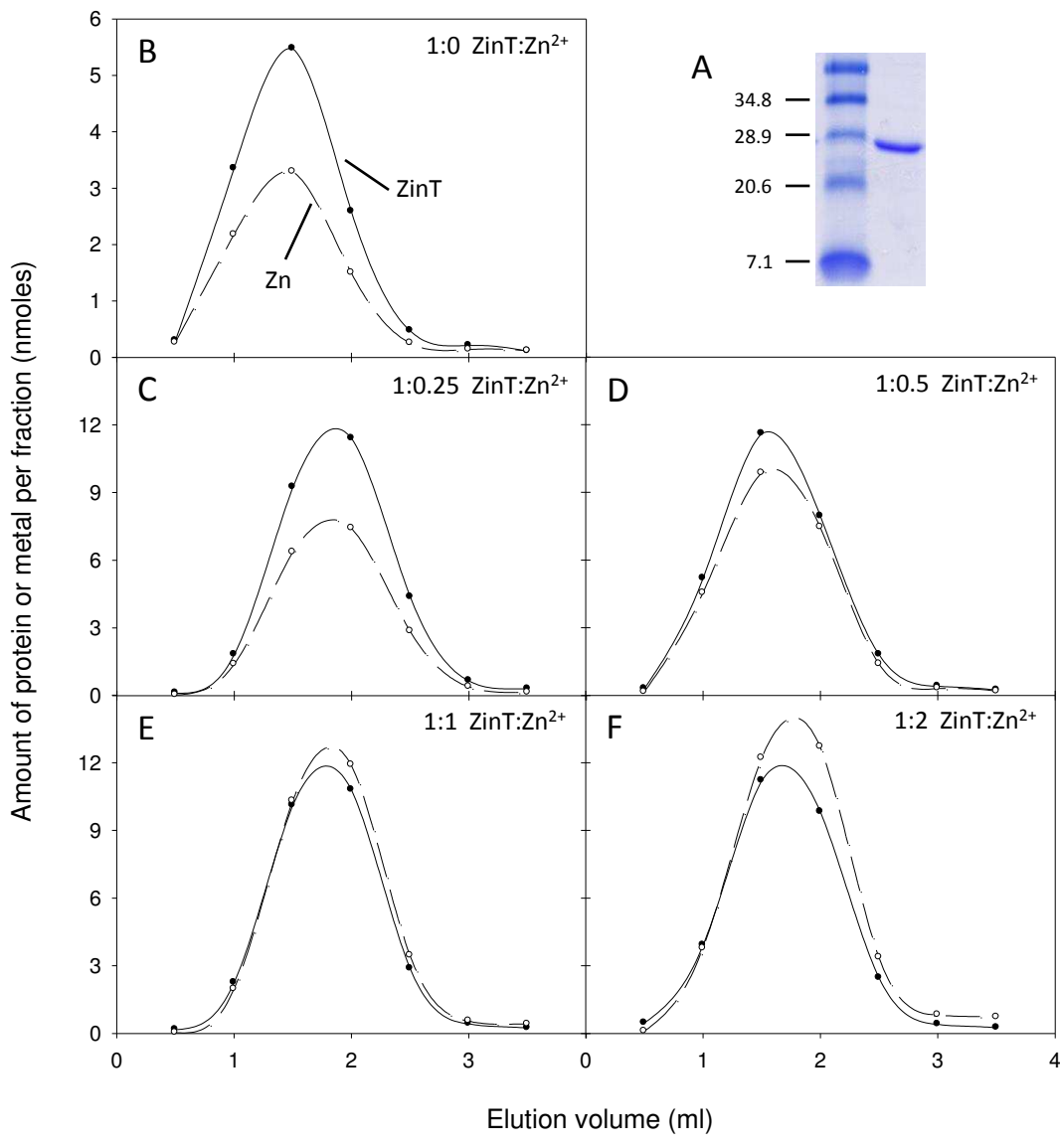


Figure 5

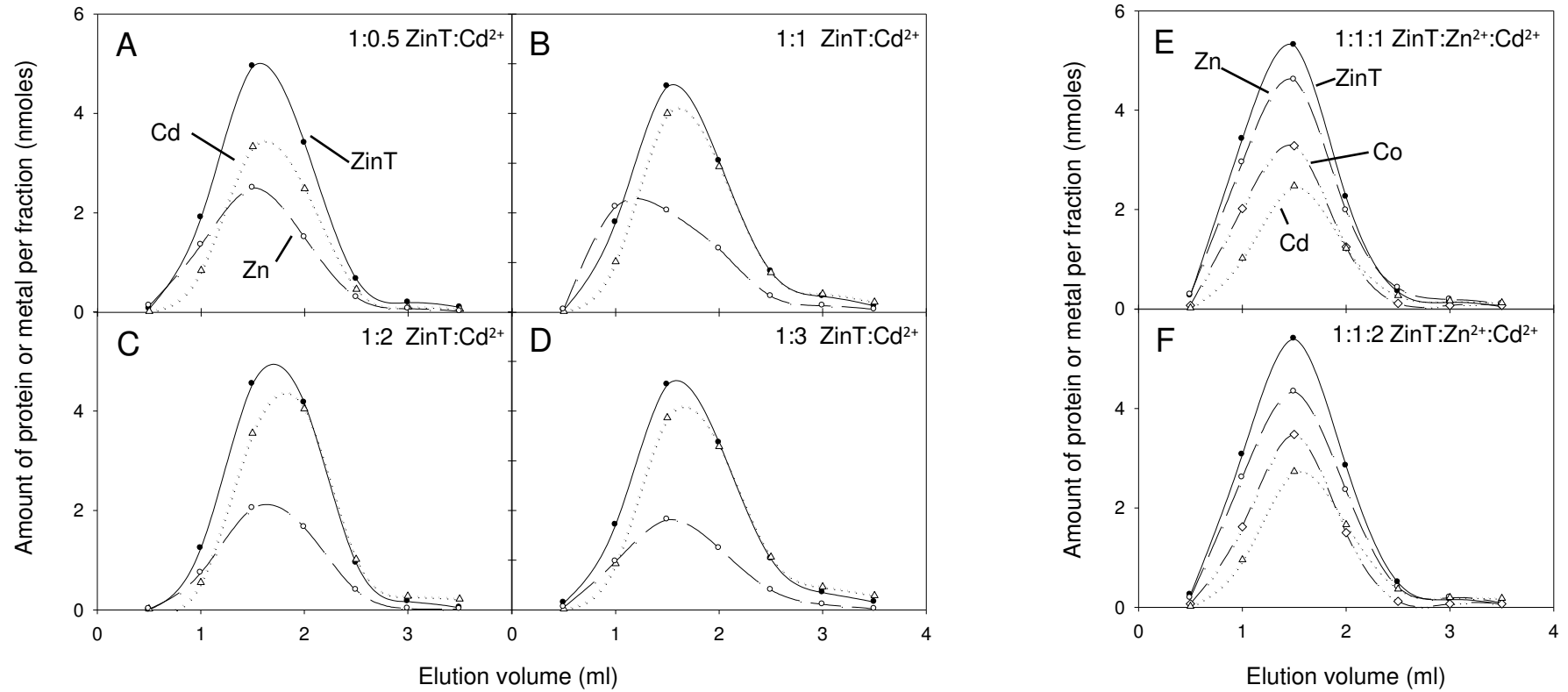


Figure 6

